TRANSIENT BEHAVIOR IN A FERRORESONANT CIRCUIT

Dunham Laboratory
Yale University
New Haven, Connecticut

TRANSIENT BEHAVIOR IN A FERRORESONANT CIRCUIT

J. G. Skalnik

Office of Naval Research, Nonr-433(00)
Report No. 8

Dunham Laboratory
Yale University
New Haven, Connecticut

Submitted: October 1954

Distribution List for Technical Reports

Office of Naval Research

2 Chief of Naval Research, Code 427, Washington

Director, Naval Research Laboratory, Washington
6 Code 2000
4 Code 2040

2 Commanding Officer, ONR, New York

1 Commanding Officer, ONR, Chicago

1 Commanding Officer, ONR, San Francisco

1 Commanding Officer, ONR, Pasadena

2 Assistant Naval Attache, ONR, London

Navy Department

Chief, Bureau of Ships, Washington
2 Code 810
1 Code 836

2 Chief, BuAer, Electronics Laboratory, Washington

1 Chief, BuOrd, Re4f, Washington

1 Director, Naval Ordnance Laboratory, White Oak

Chief of Naval Operations, Washington
1 Op-413
1 Op-32
1 Op-20

1 Director, Naval Electronics Laboratory, San Diego

U. S. Naval Academy, Post Graduate School, Monterey
1 Physics Department
1 Electronics Department

1 U. S. Navy Underwater Sound Laboratory, New London

Other Military Services

1 Chief Signal Officer, SIGET, Washington

2 Evans Signal Laboratory, Belmar

1 Commander, Wright Air Development Center
WCRDC-2

1 Commanding Officer, Watson Laboratories, Red Bank

1 Commanding Officer, Cambridge Field Station, Cambridge

1 Commandant, U. S. Coast Guard, Washington

1 Research and Development Board, Washington

1 Office of Technical Services, Washington

5 Armed Services Technical Information Agency, Dayton

Civilian

1 Massachusetts Institute of Technology, J. B. Wiesner, Cambridge

1 Massachusetts Institute of Technology, Document Room, Cambridge

1 Carnegie Institute of Technology, B. R. Teare, Pittsburgh

1 Harvard University, E. L. Chaffee, Cambridge

1 Harvard University, Phillips LeCorbeiller, Cambridge

1 Harvard University, Library, Cambridge

1 Panel on Electron Tubes, RDB, New York

1 University of Illinois, Electrical Engineering Department, Urbana

1 Stanford University, F. E. Terman, Stanford

1 Columbia University, Department of Physics, New York

1 University of California, Antenna Laboratory, Berkeley

1 University of Wisconsin, T. J. Higgins, Madison

Preface

This report is the eighth concerned with research accomplished in connection with Navy Contract Nonr-433(00), between Dunham Laboratory, Yale University, and the Office of Naval Research, Department of the Navy. In this report is given a discussion of the transient behavior of a ferroresonant circuit in the region of the steady-state response. Application of the present work to ferroresonant trigger circuits is outlined.

The research was carried on and the report written by J. G. Skalnik under the supervision of W. J. Cunningham, Director.

J. G. Skalnik

New Haven, October 1954

Table of Contents

List of Figures

List of Symbols

a	damping parameter
a_1	coefficient of linear term in series relating flux and current of inductor
a_3	coefficient of cubic term in series relating flux and current of inductor
a_5	coefficient of fifth-power term in series relating flux and current of inductor
A	general peak amplitude of solution
b	natural resonance frequency parameter in the equivalent linear case
c	nonlinearity parameter
C	capacitance
E	maximum value of applied voltage
F	peak value of excitation, $\omega_1 E$
g	factor expressing amplitude of transient component in region of lower stable state
h	factor relating frequency of transient component in region of lower stable state to the excitation frequency
i	current
L	inductance
m	amplitude-modulation index
m_0	amplitude-modulation index at $t = 0$
n	phase-modulation index
r	parameter used in determination of α
R	resistance
s	parameter used in determination of α
t	time
x	normalized response amplitude

y normalized excitation frequency

Z general angle

α number of cycles of excitation between peaks of modulation

β general phase of solution

γ phase angle of excitation

δ parameter expressing difference between the average height of the amplitude-modulation envelope and the magnitude of the steady-state solution

ε base of natural logarithm

θ angular time, radians

ϕ instantaneous value of solution, flux-linkage

ϕ_o initial value of solution

ϕ_1 average value of envelope of solution

ϕ_2 amplitude of steady-state component for high values of ϕ_o

ϕ_i amplitude of response in region of lower stable state

ϕ_s steady-state value of solution

ϕ_t amplitude of transient component for high values of ϕ_o

ψ phase angle associated with the modulation envelope

ω_1 angular frequency of excitation

ω_t angular frequency of transient component for high values of ϕ_o

Abstract

Several physical systems are described approximately by the equation

$$\frac{d^2\phi}{dt^2} + a\frac{d\phi}{dt} + b\phi + c\phi^\beta = F \cos \omega_1 t$$

where a, b and c are constants of the system and F and ω_1 are constants of the applied forcing function. This is a second-order nonlinear differential equation whose complete exact solution is unknown.

Approximate solutions for the steady-state behavior of the systems represented by the above equation are well-known. The present work investigates the transient behavior in the region of the steady-state response. The theory developed in supported by solutions using an analog computer and by experiment with an actual electrical circuit whose behavior is approximated by the above equation.

I. Introduction

The performance of many physical systems is controlled in part by a nonlinear element. Fortunately, from the point of view of simplicity of analysis, the nonlinearity is often small enough that it may be neglected without introducing appreciable error. In other cases however the nonlinearity may not be ignored and in fact may be deliberately introduced. Here an assumption that the nonlinearity is small but not negligible may lead to a mathematical expression that can be treated analytically with fair accuracy, at least in certain regions of operation. This analysis may then furnish a qualitative indication of the performance when the nonlinearity becomes more severe. In the extreme case graphical or experimental techniques may have to be employed to study the system.

Nonlinear electrical circuits that have received considerable attention in the past include those incorporating an inductor that exhibits a nonlinear relation between the flux established in the core and the current flowing in the windings on the core. Any increase of the current above a certain value leads to the establishment of very little additional flux. The inductor is then said to be saturated. One of the applications utilizing this nonlinearity has been the simulation of the effect of a mechanical relay.[1,2*] Here a slight change of a control parameter, an applied voltage for example, causes a large change in another quantity. This quantity represents the output and may be the voltage developed across one of the circuit

---

*These number symbols refer to the bibliography which appears at the end.

elements. Slight readjustment of the control parameter causes the operation to transfer back to the original state. The method of analysis used with such a circuit has been largely graphical with some attempt being made to formalize the necessary calculations using experimental data available for a particular circuit.[3] A large amount of the work reported in the literature is based on a simple series combination of resistor, capacitor, and nonlinear inductor with an a-c generator as shown in Fig. 1. However more complicated combinations have been investigated at least from a graphical point of view.[1] It should be noted that the analysis associated with the circuit of Fig. 1 is applicable to other physical systems such as those involving a nonlinear spring, nonlinear capacitor, or a synchronous machine with an oscillatory component of load.

Recently considerable interest has been shown in the circuit of Fig. 1 because of the application of so-called ferroresonant trigger circuits to electronic computers. This type of trigger circuit involves the parallel connection of two of the circuits shown in Fig. 1. This combination is then connected in series with an impedance and a source of alternating voltage.[4,5] The capacitor and the inductor in each half of the circuit would form a normal series resonant circuit at some excitation frequency if the inductor were linear. If the inductor is nonlinear however, and the frequency of excitation is increased from a low value, the condition called resonance in the linear case is only approached. Increase of the excitation frequency from a low value causes an increase in the amplitude of current flowing in the circuit. This in turn lowers the effective value of inductance

and increases the resonance frequency of the equivalent linear circuit. With further increase of the excitation frequency, the process continues with an increase of current and decrease of effective inductance. Eventually losses in the circuit will not allow the current to be increased further. Increase of the excitation frequency above this point will cause a sudden drop in the amplitude of current. The effective inductance of the circuit will return to the value existing at a low frequency of excitation. If the excitation frequency is now decreased from its high value, somewhat the same behavior is experienced except the current now suddenly jumps from a low value to a high value. This will occur at a frequency of excitation somewhat lower than that causing the sudden change of current from a high to a low value.

This behavior is typical of both halves of a ferroresonant trigger circuit but, as a consequence of the common series impedance, only one-half of the circuit may be in the high-current or high-flux state at a time. The other half at this time will be operating with a high value of effective inductance and will be drawing a relatively small current from the alternating supply. A triggering pulse applied to auxiliary windings on the cores causes the high-flux condition to switch from one inductor to the other. The design of ferroresonant trigger circuits appears to be carried out by graphical and experimental methods and little has been published about the transient behavior present during the switching interval. Isborn[4] has quoted a transfer time in the order of 5 cycles of the applied excitation voltage, and more recently Rutishauser[5] has published the figure of 3 to 4 cycles for the transfer time.

A large portion of the literature dealing with the analysis of the system represented by the circuit of Fig. 1 is concerned mainly with the steady-state response[6,7] and the regions of stability.[8] Attention has been given to developing a general method of analysis[9] but specific treatment of the transient behavior of the circuit of Fig. 1 is limited to the case of zero external excitation. Some results pertaining to the transient behavior associated with forced oscillations, that is with finite external excitation, have been published in the form of integral curves,[10] but it is difficult to interpret from these the actual time involved during a transient. Here the behavior is assumed to be in the form of the sum of two sinusoidal components, at the frequency of the excitation and 90-degrees out of phase, whose amplitudes are slowly varying functions of time. The integral curves are plots of the amplitude of one component versus the other and show clearly the effect of initial conditions in the circuit on the final operation. However numerical integration or the equivalent is required to determine the time involved in arriving at the final state and the actual waveforms existing during the time of the transient.

The present work was undertaken to investigate the transient behavior in the region of the steady-state response of the circuit of Fig. 1. The results of this analysis are applicable to the behavior of ferroresonant trigger circuits during the switching or transition interval. In particular, attention is paid to the effect of the magnitude and position in time of the triggering pulse on the transient behavior of the circuit.

As previously stated the circuit shown in Fig. 1 is one in which there exists a nonlinear relation between the flux-linkage ϕ and the current i in the iron-cored inductor. This relation may be expressed as

$$i = a_1\phi + a_3\phi^3 + a_5\phi^5 + \cdots \qquad (1)$$

where only odd-power terms appear because of the presumed symmetry of the magnetization curve about the origin. It is common practice to consider only the first two terms of this series as representing the characteristics of the inductor. Two terms allow the representation of saturation effects at large values of flux but ignore the curvature of the magnetization curve in the region of the origin. The coefficient of the linear term a_1 is the reciprocal of the usual self-inductance of a linear inductor, and the coefficient a_3 is determined by the magnitude of the nonlinearity.

The voltage equation for the circuit shown in Fig. 1 may be written as

$$\frac{d\phi}{dt} + iR + \frac{1}{C}\int i\,dt = E \sin \omega_1 t \qquad (2)$$

or by differentiation as

$$\frac{d^2\phi}{dt^2} + R\frac{di}{dt} + \frac{i}{C} = \omega_1 E \cos \omega_1 t \qquad (3)$$

where t is time, R is the resistance, C is the capacitance, ω_1 is the angular excitation frequency and E is the peak amplitude of the excitation voltage. If the relation of Eq. (1) is substituted into Eq. (3), the resulting equation is

$$\frac{d^2\phi}{dt^2} + R\frac{d}{dt}(a_1\phi + a_3\phi^3) + \frac{a_1}{C}\phi + \frac{a_3}{C}\phi^3 = \omega_1 E \cos \omega_1 t \qquad (4)$$

If the nonlinearity and the damping are considered small this may be reduced to the form

$$\frac{d^2\phi}{dt^2} + a\frac{d\phi}{dt} + b\phi + c\phi^3 = F\cos\omega_1 t \qquad (5)$$

where $a = a_1R$, $b = a_1/C$, $c = a_3/C$ and $F = \omega_1 E$. This equation is usually referred to as Duffing's[11] equation in the literature. Its complete solution is not known but it has been shown that a first approximation to the steady-state solution is[7]

$$\phi = \phi_s \cos\omega_1 t \qquad (6)$$

if the resistance term is neglected entirely. Substitution of Eq. (6) into Eq. (5) with $a = 0$, using the identity

$$\cos^3\omega_1 t = \frac{3}{4}\cos\omega_1 t + \frac{1}{4}\cos 3\omega_1 t$$

and neglecting the resulting third-harmonic term yields the relation

$$\omega_1^2 = b + \frac{3}{4}c\phi_s^2 - \frac{F}{\phi_s}. \qquad (7)$$

This relation establishes the amplitude of response ϕ_s at the fundamental frequency in relation to the circuit constants b and c and the excitation constants F and ω_1. It is of course an approximation to an exact solution because of the simplifications that have been introduced. The relation of Eq. (7) is plotted in Fig. 2 for arbitrarily-chosen values of b and F and for two values of the nonlinearity parameter, $c = 0$ and $c > 0$. The curve is a normal resonance curve of a linear circuit for $c = 0$, but for $c > 0$ the curve is tilted to the right. Since the figure is plotted for the case of zero damping, the response ϕ_s is exactly in phase with the excitation along the left-hand branch of the curves and exactly out

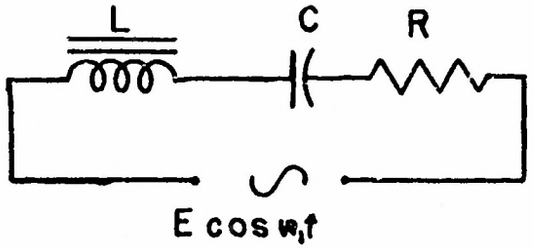

Fig. 1. Circuit with nonlinear inductor

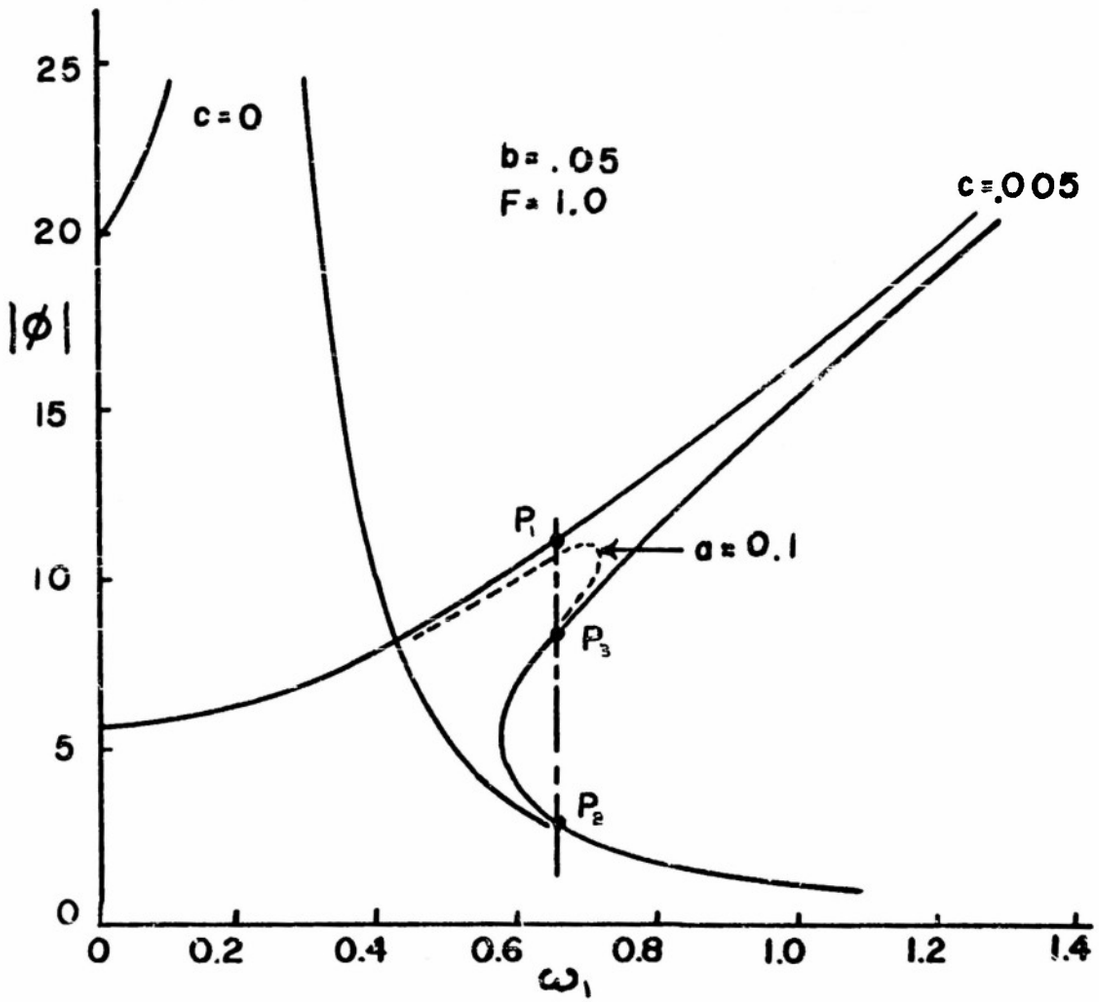

Fig. 2. Response curves for c=0 and c=.005

of phase along the right-hand branch. This must be modified slightly to include the effects of damping in the circuit but the damping is important only in a limited region so long as it is not excessive. The effect of damping on the steady-state response curve for $c > 0$ is indicated by the dotted line in Fig. 2.

It is seen that for certain values of ω_1 and for $c > 0$ there are three possible values for ϕ_s. The actual state of response depends upon past history and may be as represented by points P_1, the upper stable state, and P_2, the lower stable state. The third possible value of ϕ_s designated by P_3 is unstable[8] and any small variation from this point will cause the response to transfer to either P_1 or P_2 depending upon the nature of the disturbance.[10] The existence of these two stable states as shown in Fig. 2 is the basis for the operation of ferroresonant t_gger circuits.

If the inductor is linear, only one stable state exists for any chosen set of excitation and circuit constants. The analytical treatment for this case is fully documented in the literature.[12,13] It is established that a wide variety of transient solutions exist depending upon the initial conditions and the conditions of damping. For the case of small damping, the complete solution is in the form of the sum of two components that in general are of different frequency and amplitude. One component is sinusoidal and has the same frequency as the applied excitation and is constant in amplitude. This is the steady-state response. The other component is at a frequency dependent on the circuit constants and its amplitude decreases exponentially with time. This is the transient component. The actual appearance

of the resulting waveform varies widely depending on the relative frequency, amplitude and initial phase of the two components. If the two components are only slightly different in frequency, as would be the case when the excitation frequency is close to the natural frequency or frequency of maximum steady-state response, the resulting waveform would be expected to have regions of large amplitude where the two components [illegible]ing together almost as if they were of the same frequency and phase. This region is followed by one of small amplitude almost as if the two components were of the same frequency and in phase opposition. This is the well-known phenomenon of beating.

If one surmises that this same general sort of behavior would take place in the nonlinear case, regions of high amplitude would lead to relatively lower effective values of inductance in the circuit due to the effect of saturation and thus to a relatively higher frequency for the transient part of the solution. In a similar manner, the regions of low amplitude would lead to a relatively higher effective value of inductance in the circuit and thus to a relatively lower frequency for the transient part of the solution. This qualitative argument indicates that the situation is considerably more involved and not so easily treated analytically as the linear case. Preliminary investigations using an analog computer produced solutions of the general form shown in Sect. V, Fig. 11 which confirm the above argument. They indicate that to a first approximation the solution in a region where the nonlinearity is important may be assumed to be in the form of a sinusoid modulated both in amplitude and phase.

II. Transient Behavior in the Region of the Upper Stable State

1. General undamped case.

In this section the behavior of an undamped system described by Eq. (5) with $a = 0$ and operating in the neighborhood of the upper stable state is investigated. The equation describing the operation is then

$$\frac{d^2\phi}{dt^2} + b\phi + c\phi^3 = F \cos \omega_1 t \tag{5a}$$

If the substitution of $\theta = \omega_1 t$ is made, Eq. (5a) becomes

$$\frac{d^2\phi}{d\theta^2} + \frac{b}{\omega_1^2}\phi + \frac{c}{\omega_1^2}\phi^3 = \frac{F}{\omega_1^2} \cos \theta \tag{5b}$$

The solution of Eq. (5b) is assumed to be of the form

$$\phi = A \cos \beta \tag{8}$$

where in general A and β are functions of θ and are described more fully later. By differentiation of Eq. (8)

$$\frac{d\phi}{d\theta} = -A \sin \beta \frac{d\beta}{d\theta} + \cos \beta \frac{dA}{d\theta} \tag{9}$$

and in a similar manner

$$\frac{d^2\phi}{d\theta^2} = -A \sin \beta \frac{d^2\beta}{d\theta^2} - A \cos \beta \left(\frac{d\beta}{d\theta}\right)^2 - 2 \sin \beta \frac{d\beta}{d\theta}\frac{dA}{d\theta} + \cos \beta \frac{d^2A}{d\theta^2} \tag{10}$$

It is also seen that

$$\phi^3 = A^3 \cos^3 \beta = A^3\left(\frac{3}{4} \cos \beta + \frac{1}{4} \cos 3\beta\right) \tag{11}$$

As in the introduction the third harmonic term is neglected here and thus, approximately

$$\phi^3 = \frac{3}{4} A^3 \cos \beta \tag{11a}$$

The neglect of the third harmonic term precludes the possibility of obtaining an exact solution to Eq. (5b) by the following development.

Thus any solution in the form of a sinusoid gained in the present analysis represents only the fundamental term of the waveform that would be determined experimentally in an actual circuit. In particular, as may be seen by inspection of Eq. (11), the neglected third-harmonic term would lead to a triangular-shaped waveform of flux. Differentiation of Eq. (11) leads to the expectation of a flat-topped waveform of voltage for the inductor in the actual circuit of Fig. 1.

By substituting Eqs. (8), (10) and (11a) into Eq. (5b) it is seen that

$$-A \sin\beta \frac{d^2\beta}{d\theta^2} - A \cos\beta \left(\frac{d\beta}{d\theta}\right)^2 - 2 \sin\beta \frac{d\beta}{d\theta}\frac{dA}{d\theta} + \cos\beta \frac{d^2A}{d\theta^2}$$

$$- \frac{F}{\omega_1^2} \cos(\theta + \gamma) + \frac{b}{\omega_1^2} A \cos\beta + \frac{3}{4}\frac{c}{\omega_1^2} A^3 \cos\beta = 0 \qquad (12)$$

where the angle γ has been included in the argument of the excitation function to allow an arbitrary phase of excitation at $t = 0$. This is equivalent to allowing the triggering pulse in a ferroresonant trigger circuit to occur at any time in the excitation voltage cycle. It is presumed in the following analysis that the pulsing circuit can completely determine the flux to be ϕ_o at $\theta = 0$, hold the rate of change of flux at zero at the time $\theta = 0$, and then release the system in a zero time interval to react according to the equations to be developed. In an actual trigger circuit, the pulse is introduced as a voltage pulse or current pulse rather than a pulse of flux directly. In either case however, the application of the pulse to windings on the core of the inductor results in flux being established in the core. Thus it is assumed that the waveform of the voltage

or current pulse is adjusted to satisfy the desired initial condition of flux. As a practical matter, the presumed initial conditions put rather rigid requirements on the triggering pulse in a ferroresonant trigger circuit and it is probably difficult to satisfy these requirements exactly.

Following the argument in the introduction, the amplitude A in the above solution, Eq. (8), is assumed to be of the form

$$A = \phi_1\left[1 + m \sin\left(\frac{\theta}{\alpha} + \psi\right)\right] \tag{13}$$

where m is the amplitude-modulation index, α is the number of cycles of the excitation existing between successive peaks of the modulation, ϕ_1 is the average amplitude and ψ is the phase angle associated with the envelope. The phase function is assumed to be of the form

$$\beta = \theta + \gamma - n \cos\left(\frac{\theta}{\alpha} + \psi\right) \tag{14}$$

where n is the phase-modulation index. Then the following relations are valid.

$$\frac{dA}{d\theta} = \phi_1 \frac{m}{\alpha} \cos\left(\frac{\theta}{\alpha} + \psi\right) \tag{15}$$

$$\frac{d^2A}{d\theta^2} = -\phi_1 \frac{m}{\alpha^2} \sin\left(\frac{\theta}{\alpha} + \psi\right) \tag{16}$$

$$\frac{d\beta}{d\theta} = 1 + \frac{n}{\alpha} \sin\left(\frac{\theta}{\alpha} + \psi\right) \tag{17}$$

$$\frac{d^2\beta}{d\theta^2} = \frac{n}{\alpha^2} \cos\left(\frac{\theta}{\alpha} + \psi\right) \tag{18}$$

If the value of m is kept reasonably small as compared to unity, the terms involving m of power higher than two may be neglected. Thus

$$A^3 = \phi_1^3\left[1 + m \sin\left(\frac{\theta}{\alpha} + \psi\right)\right]^3 \simeq \phi_1^3\left[1 + \frac{3}{2} m^2 + 3 m \sin\left(\frac{\theta}{\alpha} + \psi\right)\right], \tag{19}$$

Equation (19) is obtained by using the identity $\sin^2 Z = \frac{1}{2}\left[1 - \cos 2Z\right]$ and neglecting the term which leads to a second harmonic in the envelope of the solution. In a similar manner

$$\left(\frac{d\beta}{d\theta}\right)^2 = 1 + \frac{2n}{\alpha} \sin\left(\frac{\theta}{\alpha} + \psi\right) + \frac{n^2}{2\alpha^2} \tag{20}$$

Use is also make of the series form of the sine and cosine functions where

$$\cos Z = 1 - \frac{Z^2}{2} + \frac{Z^4}{24} \cdot \cdot \cdot \cdot \cdot \tag{21}$$

and

$$\sin Z = Z - \frac{Z^3}{6} + \frac{Z^5}{120} \cdot \cdot \cdot \cdot \tag{22}$$

If the terms higher than the squared term are neglected

$$\cos \beta = \left(1 - \frac{n^2}{4}\right) \cos(\theta + \gamma) - n \sin\left(\frac{\theta}{\alpha} + \psi\right) \cos(\theta + \gamma) \tag{23}$$

and

$$\sin \beta = \left(1 - \frac{n^2}{4}\right) \sin(\theta + \gamma) + n \sin\left(\frac{\theta}{\alpha} + \psi\right) \cos(\theta + \gamma) \tag{24}$$

where the trigonometric identities of the form

$$\cos(W + Z) = \cos W \cos Z - \sin W \sin Z \tag{25}$$

and

$$\sin(W + Z) = \sin W \cos Z + \cos W \sin Z \tag{26}$$

have been utilized and again the second-harmonic terms arising from the Z^2 term have been neglected.

If Eqs. (13) through (24), with the simplifications as outlined, are inserted in Eq. (12), the expression expanded by simple multiplication and the terms collected, the result is

$$\left(-1 - \frac{F}{\phi_1 \omega_1^2} + \frac{b}{\omega_1^2} + \frac{3c\phi_1^2}{4\omega_1^2} + \frac{n^2}{4} - \frac{n^2 b}{4\omega_1^2} - \frac{3c\phi_1^2 n^2}{16\,\omega_1^2} + \frac{9cm^2\phi_1^2}{8\,\omega_1^2}\right) \cos(\theta + \gamma)$$

$$+ \left(n - \frac{bn}{\omega_1^2} - \frac{3cn\phi_1^2}{4\,\omega_1^2} + \frac{n}{a^2} + \frac{2m}{a}\right) \cos\left(\frac{\theta}{a} + \psi\right) \sin(\theta + \gamma)$$

$$+ \left(-m + \frac{bm}{\omega_1^2} + \frac{9cm\phi_1^2}{4\,\omega_1^2} - \frac{m}{a^2} - \frac{2n}{a}\right) \cos(\theta + \gamma) \sin\left(\frac{\theta}{a} + \psi\right) = 0 \qquad (27)$$

where, as before, the terms of the multiplication process leading to a second harmonic in the solution and the terms in n and m higher than the second power have been neglected. From this expression it is seen that

$$-1 - \frac{F}{\phi_1 \omega_1^2} + \frac{b}{\omega_1^2} + \frac{3c\phi_1^2}{4\omega_1^2} + \frac{n^2}{4} - \frac{n^2 b}{4\omega_1^2} - \frac{3c\phi_1^2 n^2}{16\,\omega_1^2} + \frac{9cm^2\phi_1^2}{8\,\omega_1^2} = 0 \qquad (28)$$

$$n - \frac{bn}{\omega_1^2} - \frac{3cn\phi_1^2}{4\,\omega_1^2} + \frac{n}{a^2} + \frac{2m}{a} = 0 \qquad (29)$$

and

$$-m + \frac{bm}{\omega_1^2} + \frac{9cm\phi_1^2}{4\omega_1^2} - \frac{m}{a^2} - \frac{2n}{a} = 0 \qquad (30)$$

since the trigonometric forms in Eq. (27) are not in general zero. For simplicity the following two definitions are made.

$$r \equiv -1 + \frac{b}{\omega_1^2} + \frac{9c\phi_1^2}{4\,\omega_1^2}$$

$$s \equiv -1 + \frac{b}{\omega_1^2} + \frac{3c\phi_1^2}{4\,\omega_1^2}$$

Now Eqs. (29) and (30) may be rewritten as

$$-n\left(s - \frac{1}{\alpha^2}\right) + \frac{2m}{\alpha} = 0 \tag{29a}$$

and

$$m\left(r - \frac{1}{\alpha^2}\right) - \frac{2n}{\alpha} = 0 \tag{30a}$$

By combining these two equations to eliminate m and n it follows that

$$(r\alpha^2 - 1)(s\alpha^2 - 1) = 4\alpha^2 \tag{31}$$

or

$$\alpha^2 = \frac{(r + s + 4) + \sqrt{(r + s + 4)^2 - 4rs}}{2\,rs} \tag{31a}$$

To establish the boundary conditions at zero time, two expressions are necessary to satisfy the initial amplitude ϕ_o and the initial slope, $\frac{d\phi}{d\theta}$ at $\theta = 0$, of the solution. If an amplitude ϕ_o is introduced in the system at zero time,

$$\phi_o = \phi_1 (1 + m \sin \psi) \cos (\gamma - n \cos \psi) \tag{32}$$

This relation is gained by combining Eqs. (8), (13) and (14) at $\theta = 0$. If the initial conditions allow $\frac{d\phi}{d\theta}$ to be zero at $\theta = 0$, Eqs. (9), (13), (14), (15) and (17) may be combined to give the relation

$$\tan (\gamma - n \cos \psi) = \frac{\frac{m}{\alpha} \cos \psi}{(1 + m \sin \psi)\left(1 + \frac{n}{\alpha} \sin \psi\right)} \tag{33}$$

2. Case of introducing the triggering pulse of flux at the time of the peak of the excitation.

As stated in the introduction the steady-state flux for the undamped case is either in phase or out of phase with the excitation

voltage. Thus if the operation is in a region where two stable states exist and the flux has a magnitude consistent with the lower state, a pulse of flux of the form previously described and of positive polarity should be introduced at the time of the positive peak of the excitation to cause the operation to transfer to the upper stable state. If this pulse is of exactly the correct magnitude consistent with the upper stable state and releases the system with $\frac{d\phi}{dt} = 0$, no transient will be generated. If the operation is initially at the upper stable state, a negative pulse should be introduced at the time of the positive peak of the excitation to transfer operation to the lower stable state.

For the simplest possible situation it is assumed that the value of α is large, greater than ten for example, so the terms involving $\frac{d^2A}{d\theta^2}$ and $\frac{d^2\beta}{d\theta^2}$ in Eq. (12) may be neglected. This may be verified by the comparison of Eqs. (15) and (16), and by the comparison of Eqs. (17) and (18). It might be observed at this point that Hayashi[10] has neglected the equivalent of these second-derivative terms throughout his analysis. All but the linear terms in n and m are neglected here and since the pulse is to be introduced as just the proper time, $\gamma = 0$. Under these simple conditions Eqs. (28), (29) and (30) reduce to

$$-1 - \frac{F}{\phi_1 \omega_1^2} + \frac{b}{\omega_1^2} + \frac{3c\phi_1^2}{4\omega_1^2} = 0 \qquad (28b)$$

$$-ns + \frac{2m}{\alpha} = 0 \qquad (29b)$$

$$mr - \frac{2n}{\alpha} = 0 \qquad (30b)$$

and Eq. (31a) becomes

$$\alpha^2 = \frac{4}{rs} \tag{31b}$$

where r and s are the same quantities as previously defined. Equation (28b) indicates that ϕ_1, the average amplitude or the average height of the envelope of the solution, is identical with ϕ_s, the value of the upper stable solution discussed in the introduction and given by Eq. (7). Since n and m must carry the same algebraic sign to cause the regions of high amplitude to correspond to the regions of high frequency in the waveform of the solution, it can be seen from Eq. (33) with $\gamma = 0$ that either n and m must be zero or $\cos \psi$ must be zero. Since it is known that in general n and m are not zero, it is concluded that $\psi = 90^\circ$. By substitution of $\gamma = 0$, $\psi = 90^\circ$ and $\phi_1 = \phi_s$ in Eq. (32),

$$\phi_o = \phi_s (1 + m) \tag{32a}$$

and thus the relative amplitude modulation is determined entirely by the magnitude of the pulse inserted in the system so long as m is not allowed to become so large as to make the assumptions used in the derivation invalid. The phase modulation of the solution may be computed by combining Eqs. (29b), (30b) and (31b) to achieve

$$n = m\sqrt{\frac{r}{s}} \tag{34}$$

Experience has shown that the value for α is often less than ten for many physical systems so the neglect of the second-derivative terms introduces appreciable error. If these terms are retained but the terms in n^2 and m^2 are still neglected, the resulting expressions are

$$\phi_o = \phi_s (1 + m) \tag{32a}$$

$$\alpha^2 = \frac{(r + s + 4) + \sqrt{(r + s + 4)^2 - 4\,rs}}{2\,rs} \tag{31a}$$

and

$$n = \frac{\alpha m}{2} \left(r - \frac{1}{\alpha^2}\right) \tag{34a}$$

Here the relative amplitude modulation is still determined by the magnitude of the pulse, but α is related to r and s, and n is related to m, by more complicated expressions. From these equations the waveform of the complete solution consistent with the assumptions involved may be computed. For computational purposes it is convenient to normalize the curves of Fig. 2 to include all possible values of the parameters. For this purpose the ϕ_s in Eq. (7) is related to a parameter x by

$$\phi_s \equiv \left(\frac{F}{c}\right)^{1/3} x \ .$$

Then

$$\omega_1^2 = b + \frac{3}{4}\, c \left(\frac{F}{c}\right)^{2/3} x^2 - \frac{F}{\left(\frac{F}{c}\right)^{1/3} x} \tag{7b}$$

By dividing through by b and rearranging terms

$$\left(\frac{\omega^2}{b} - 1\right) = \frac{3}{4} \frac{c^{1/3} F^{2/3}}{b} x^2 - \frac{F^{2/3} c^{1/3}}{bx} \tag{7c}$$

or upon dividing through by $\dfrac{c^{1/3} F^{2/3}}{b}$ and letting

$$y = \left(\frac{\omega_1^2}{b} - 1\right) \frac{b}{F^{2/3} c^{1/3}}$$

it is determined that

$$y = \frac{3}{4} x^2 - \frac{1}{x} \tag{7d}$$

where y is the normalized excitation frequency and x is the normalized stable response amplitude. Equation (7d) is plotted as the

solid curve in Fig. 3. Once the circuit constants and the drive or excitation constants have been selected for a particular system the position along the abscissa is established. This allows the direct reading of the normalized response magnitude, and this can be converted to actual response since the normalizing factors along the ordinate are now known. Lines of constant α and lines of constant m according to Eq. (31a) and (32a) respectively are shown in Fig. 3. Numerical values for the contours of constant α on this chart depend upon the circuit constants in a complicated manner and thus are not universal. However by substitution of the definitions of x and y into the definitions of r and s, and elimination of y by the use of Eq. (7d), it can be shown that

$$\left(\frac{\omega_1^2}{c^{1/3} F^{2/3}}\right) r = \frac{3}{2} x^2 + \frac{1}{x} \tag{35}$$

and

$$\left(\frac{\omega_1^2}{c^{1/3} F^{2/3}}\right) s = \frac{1}{x} \tag{36}$$

These relations are plotted in Fig. 4 so the actual r and s may be obtained quickly once the circuit and excitation constants are known. After r and s have been determined, the numerical value of α is established through the application of Eq. (31a). This relation is plotted in Fig. 5 with α as a parameter.

3. Case of introducing the triggering pulse of flux at the correct time and including n^2 and m^2 terms.

The equations pertaining to this situation are those derived in Section II. 1. with $\gamma = 0$ and $\psi = 90$ degrees. However it can be

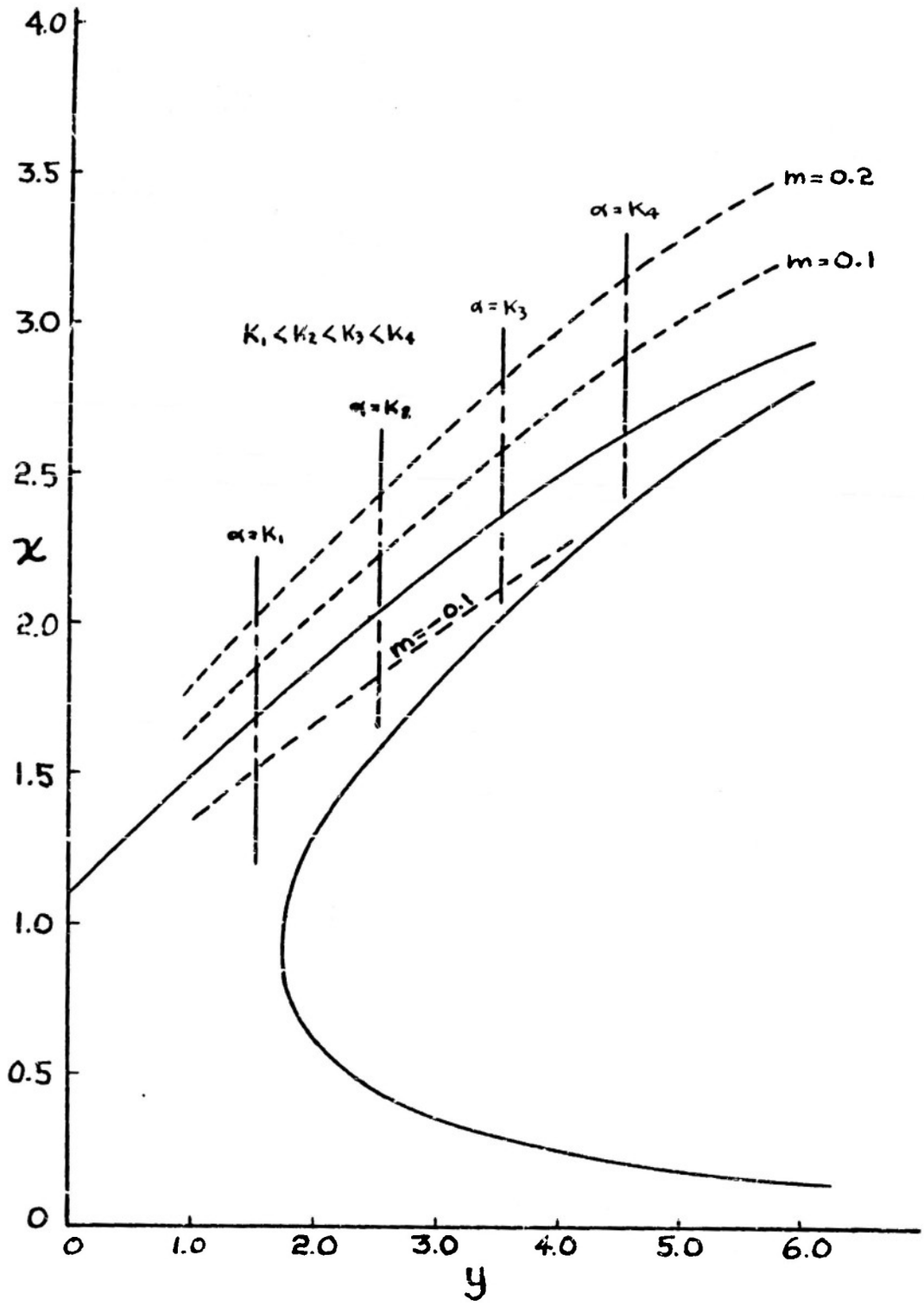

Fig. 3. Normalized response curve

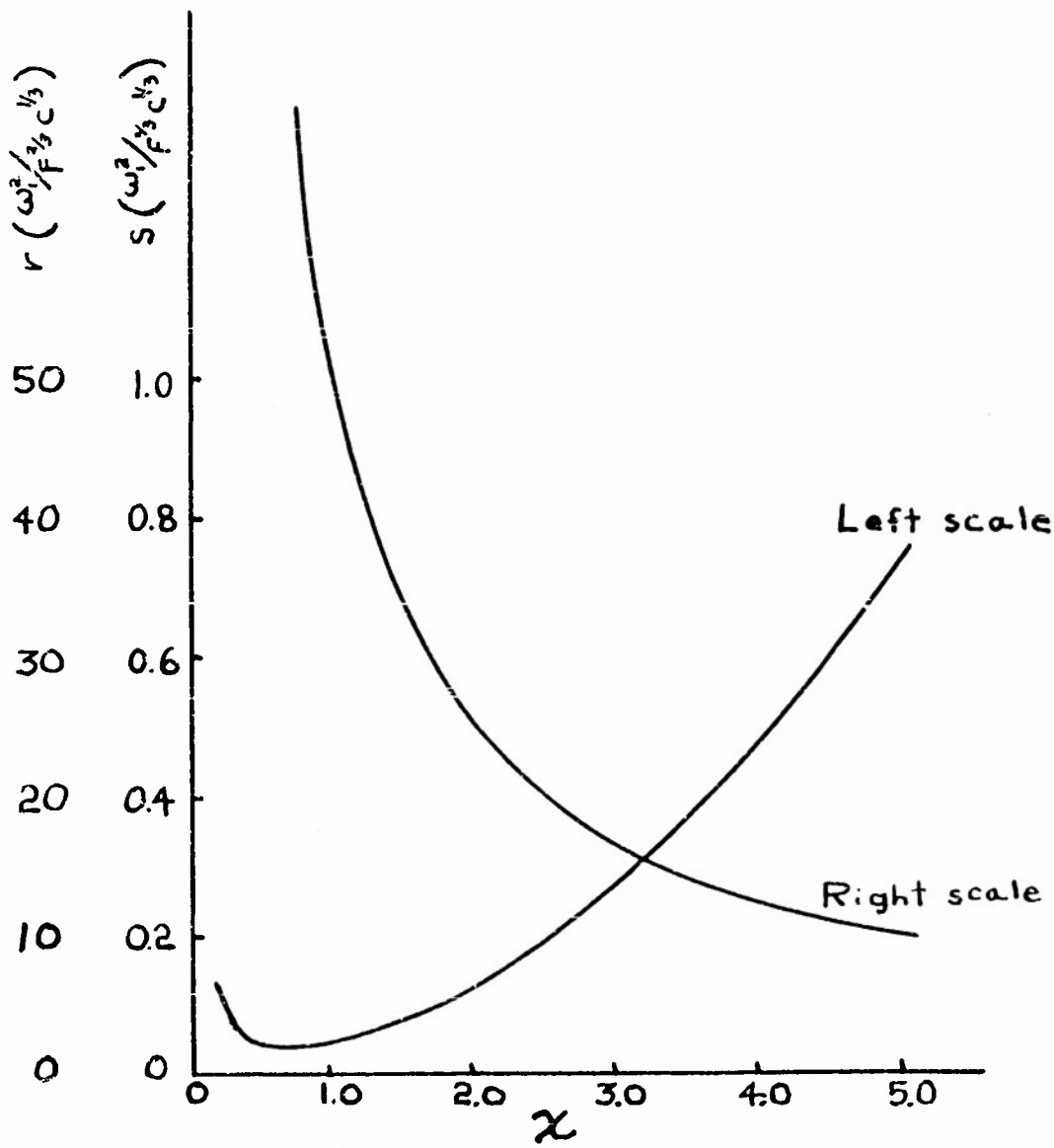

Fig. 4. Curves for determination of r and s

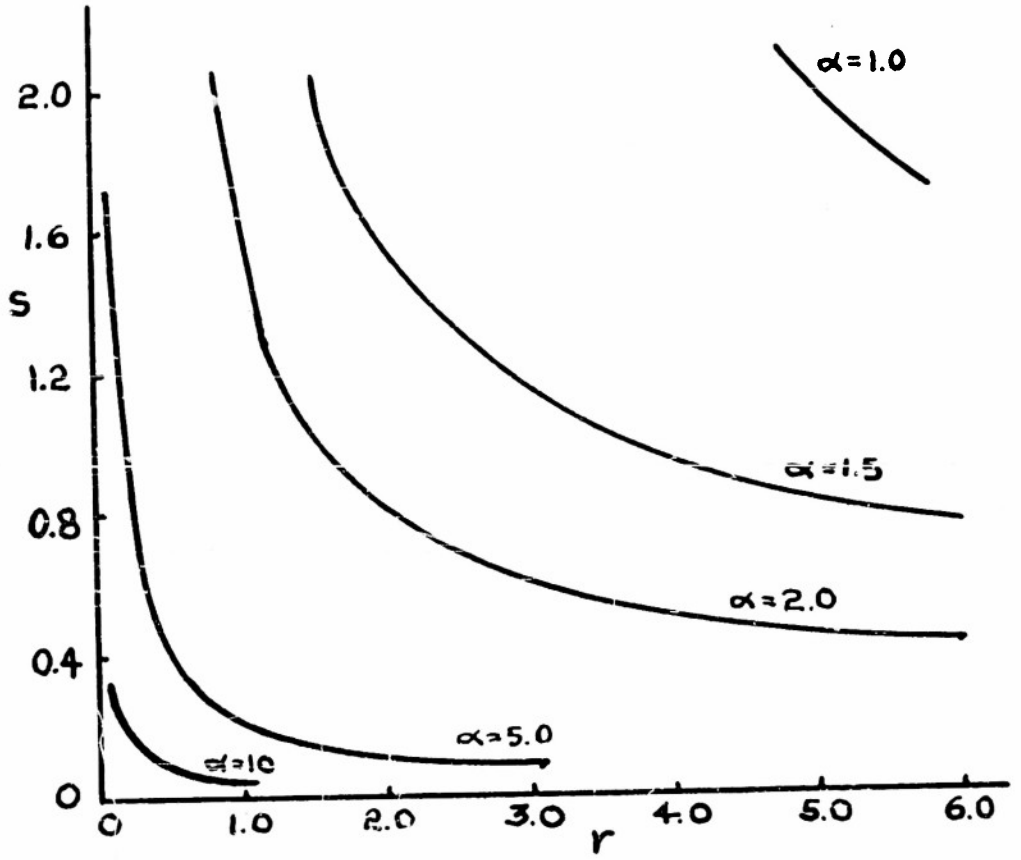

Fig. 5. Curves for determination of α.

seen from Eq. (28) that the average value of the envelope of the solution ϕ_1 is no longer equal to the stable solution ϕ_s as in the simple case considered in Section II. 2. This is a consequence of the constant terms introduced along with the second-harmonic terms in the analysis of Section II. 1.

To use these complete equations one must resort to reasonably involved numerical calculations. The results of such a calculation are shown in Fig. 6 for $b = .05$, $c = .005$ and $F = 1.0$. The general method of calculation is to let $\phi_1 = \delta\phi_s$ and then assign the parameter δ various values. This allows the calculation of r and s and thus the determination of α. By combining Eqs. (28), (29a) and (30a) it is seen that

$$m^2\left[\frac{9c\delta^2\phi_s^2}{8\omega_1^2} - \frac{s\alpha^2}{16}\left(r - \frac{1}{\alpha^2}\right)^2\right] = \frac{F}{\delta\phi_s\omega_1^2} - s \qquad (35)$$

This equation is used to calculate the value of m. Since $\gamma = 0$ and $\psi = 90$ degrees, Eq. (32) may be written as

$$\phi_o = \phi_1(1 + m) = \delta\phi_s(1 + m) \qquad (32b)$$

and this equation is then used to calculate the value of ϕ_o required to produce the assumed condition of modulation. By selecting a sufficient number of values for δ the contours of constant α as shown in Fig. 6 may be established. These contours have not been extended below the steady-state response curve but this may easily be done since m appears as a squared term in Eq. (35) and only positive values have been considered in the plotting of the constant α contours in Fig. 6. Use of the negative values of m in Eq. (32b) leads to the

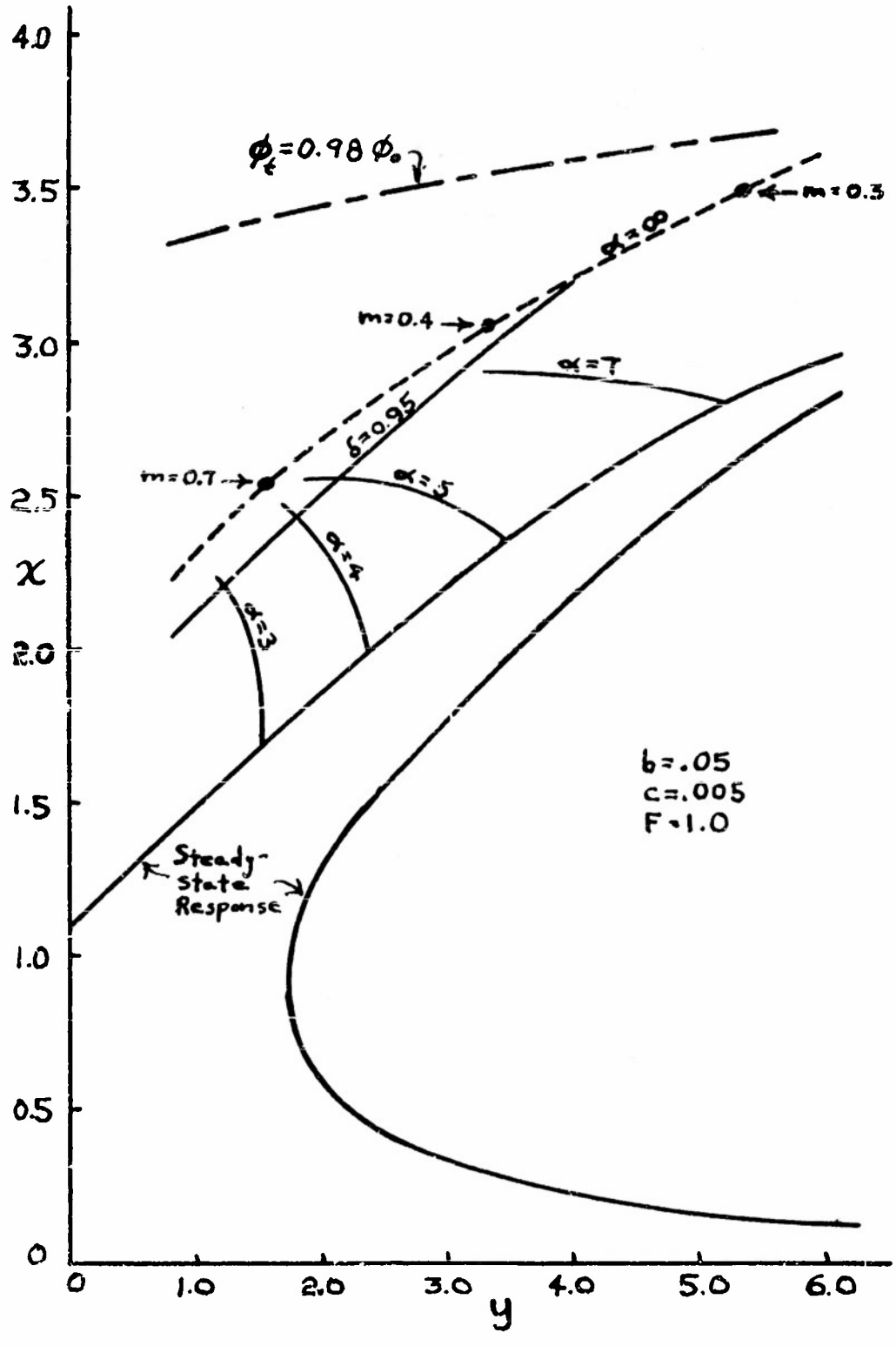

Fig. 6. Curves illustrating effect of including n^2 and m^2 terms

contours of constant α in Fig. 6 passing through the steady-state response curve and proceeding downward and to the left.

By comparison of Fig. 6 with Fig. 3, the effect of the inclusion of the n^2 and m^2 terms may be seen. The contours of constant δ, which correspond qualitatively to contours of constant error in the solution given in Section II. 2. where n^2 and m^2 terms have been neglected, lie more nearly parallel to the stable solution curve than do the contours of constant m of Fig. 3. The contour for $\delta = 0.95$ is labelled in Fig. 6 and the left-hand branch of the steady-state response curve is the contour for $\delta = 1.0$. Also as ϕ_o is increased in magnitude from that which would lead to a transient-free solution, the value of α actually increases somewhat. These equations and Fig. 6 indicate that α goes to infinity but due to the assumptions made in the analysis, the equations are not valid in this region, since m is no longer small as compared to unity. Values of m at several points along the $\alpha = \infty$ contour are shown in Fig. 6. To achieve a closer approximation more of the higher-power terms would have to be included in the analysis. This leads to extremely unwieldly expressions.

The contour for $\alpha = \infty$, shown as a dotted line in Fig. 6, consistent with the present assumptions can readily be calculated. For α to approach infinity, r or s must approach zero and thus Eq. (31a) reduces to

$$\alpha^2 \approx \frac{s + r + 4}{rs} \approx \frac{r + 4}{rs} \tag{31c}$$

since the term of $4rs$ is no longer important. Comparison of the definitions of r and s indicate that s becomes zero before r

does as δ is decreased from unity. Substituting the value of $\alpha^2 s$ calculated from the above equation into Eq. (35) with $s = 0$ and $\alpha = \infty$ yields

$$m^2\left[\frac{9c\delta^2\phi_s^2}{8\omega_1^2} - \frac{r(r+4)}{16}\right] = \frac{F}{\delta\phi_s\omega_1^2} \tag{35a}$$

By replacing ϕ_1 by $\delta\phi_s$, the definition of s may be rewritten as

$$s \equiv -1 + \frac{b}{\omega_1^2} + \frac{3c\delta^2\phi_s^2}{4\omega_1^2}$$

Since s is now zero, the value of δ may be calculated from this equation once the circuit and excitation constants are chosen. This value of δ is then substituted in Eq. (35a) to allow the calculation of m and thus ϕ_o by the use of Eq. (32b). This establishes the $\alpha = \infty$ contour shown in Fig. 6. As already mentioned this value of α does not actually exist but instead, as experiment has shown, α has increased only moderately from its value for $m \ll 1.0$, and m is close to unity at this boundary.

The calculations of this section have indicated the effect of including the n^2 and m^2 terms in the analysis. It should be noted that the calculations were based on a particular circuit and thus the numbers appearing are not universal. However the trends indicated in Fig. 6 may be generally useful. This section also indicates that the difficulty of calculation increases rapidly as the next higher-order terms are included in the analysis.

4. Operation with large values of ϕ_o.

Experiments using an analog computer have indicated that the solution is controlled almost entirely by a high-frequency transient for values of ϕ_o larger than that given by the $\alpha = \omega$ contour in Fig. 6. In this case it is assumed that the solution has the form

$$\phi = \phi_2 \cos \omega_1 t + \phi_t \cos \omega_t t \tag{36}$$

where ϕ_2 is the amplitude of the component at the frequency of the excitation ω_1, and ϕ_t is the amplitude of the transient component at the frequency ω_t. By successive differentiation, cubing, neglect of third-harmonic terms, substitution into Eq. (5a), and collection of terms, it is found that

$$-\omega_1^2 + b + \frac{3}{4} c \phi_2^2 + \frac{3}{2} c \phi_t^2 - \frac{F}{\phi_2} = 0 \tag{37}$$

and

$$-\omega_t^2 + b + \frac{3}{2} c \phi_2^2 + \frac{3}{4} c \phi_t^2 = 0 \tag{38}$$

To satisfy the boundary conditions at $t = 0$

$$\phi_o = \phi_2 + \phi_t \tag{39}$$

Eliminating ϕ_2 from Eq. (37) by the use of Eq. (39), the following equation is gained:

$$-\omega_1^2 + b + \frac{3}{4} c (\phi_o - \phi_t)^2 + \frac{3}{2} c \phi_t^2 - \frac{F}{\phi_o - \phi_t} = 0 \tag{40}$$

Knowing the circuit and drive constants, the value of ϕ_t may be calculated consistent with various values of the initial condition ϕ_o. This allows the calculation of ϕ_2 by means of Eq. (39) and thus the calculation of ω_t using Eq. (38).

If the component ϕ_2 is allowed arbitrarily to be 2% and thus ϕ_t to be 98% of ϕ_o, a boundary may be established above which the

solution is controlled almost entirely by the transient. Such a boundary is shown as the upper dashed curve in Fig. 6 for the constants $b = .05$, $c = .005$ and $F = 1.0$. Below this boundary, but above the contour labelled $\alpha = \infty$, the approximate waveform of the solution may be found by calculation of the ratio $\frac{\phi_t - \phi_2}{\phi_t + \phi_2}$ to establish the peak-to-peak variation in the solution. The approximate time interval between these peaks may be computed by the comparison of ω_t and ω_1.

5. Case of $\phi_o = \phi_s$ and $\gamma \neq 0$.

This is the situation existing when the triggering pulse of flux in a ferroresonant trigger circuit is of the correct amplitude, that is the amplitude consistent with the upper stable-state response, but where it is introduced in the system other than at the time of the positive peak of the excitation voltage.

For simplicity the calculations here are carried out with the neglect of the n^2 and m^2 terms. The equations (28b), (29a) and (30a) are then valid and the average value of the envelope of the solution is again equal to ϕ_s. If the argument of the tangent function in Eq. (33) is assumed to be small and m and n are still restricted to be reasonably small as compared to unity, the angle $(\gamma - n \cos \psi)$ in Eq. (33) is approximately equal to $\frac{m}{\alpha} \cos \psi$. Substitution of this approximate equality into Eq. (32) with $\phi_o = \phi_1 = \phi_s$ leads to the requirement that $\psi = 0$ if m is not restricted to zero for this condition of operation. Thus Eq. (32) reduces to

$$\phi_s = \phi_s \cos (\gamma - n) \qquad (32b)$$

This indicates that $n = \gamma$. In the case where the n^2 and m^2 terms are retained, ϕ_1 is not quite equal to ϕ_s and correspondingly n is not quite equal to γ. However if γ is not allowed to become large, the present equations represent a good approximation. Contours of constant m and constant α are shown in Fig. 7 for the constants $b = .05$, $c = .005$ and $F = 1.0$. The abscissa is the normalized frequency and the ordinate is the angle γ in radians. The value of α was calculated using Eq. (31a) and the value of m calculated by using Eq. (30a).

6. Case of $\phi_o \neq \phi_s$ and $\gamma \neq 0$.

Previous sections have shown that the undamped solution in the neighborhood of the upper stable region is in the form of a sinusoid modulated both in amplitude and phase. If $\gamma = 0$ but $\phi_o \neq \phi_s$, the modulation depends to a first approximation on the ratio ϕ_o/ϕ_s. If $\phi_o = \phi_s$ but $\gamma \neq 0$, the modulation depends to a first approximation on γ. However in the general case, $\phi_o \neq \phi_s$ and $\gamma \neq 0$. In other words, the triggering pulse of flux is of the wrong amplitude and is introduced at the wrong time in the excitation cycle. As indicated in the previous sections both of these inequalities lead to modulation in amplitude and phase.

In the treatment of this general case, the n^2 and m^2 terms are neglected so Eqs. (28b), (29a), (30a), (31a), (32) and (33) are valid, $\phi_1 = \phi_s$ and $0 \leq \psi \leq 90^\circ$. Thus Eq. (32) and Eq. (33) do not reduce to any simple form and calculations are more laborious than in the other cases. To indicate graphically the nature of the above

equations a sample calculation was made for $b = .05$, $c = .005$, $F = 1.0$ and $\omega_1 = 0.6$. These quantities determine r and s and thus α may be calculated by the use of Eq. (31a). The $m = 0.1$ contour as shown in Fig. 8 was calculated by solving for n using Eq. (30a) and putting this value for n and the assumed value of $m = 0.1$ into Eq. (33) which is then a transcendental equation in γ and ψ. By a trial-and-error process, values of ψ were determined for various assumed values of γ. These values were then inserted in Eq. (32) to obtain the allowable value of ϕ_o/ϕ_s which is then used as the abscissa in Fig. 8. This figure indicates the combinations of γ and ϕ_o/ϕ_s that will lead to an amplitude-modulation index of 0.1 for the particular circuit and drive constants given above.

III. Transient Behavior in the Region of the Lower Stable State.

In the undamped case the operation is determined by the equation

$$\frac{d^2\phi}{d\theta^2} + \frac{b}{\omega_1^2} + \frac{c}{\omega_1^2}\phi^3 = \frac{F}{\omega_1^2}\cos\theta \qquad (5b)$$

It can be seen by a comparison of the two curves of Fig. 2 that the nonlinearity is generally not so important in the region of the lower stable state as it is in the region of the upper stable state. Analog computer plots as shown in Section V, Fig. 14 confirm this statement. Therefore it is assumed that the solution is of the form

$$\phi = \phi_\ell\left(\cos\theta + g\cos\frac{\theta}{n}\right) \qquad (41)$$

This is the sum of two cosinusoidal components of amplitude ϕ_ℓ and $g\phi_\ell$, respectively, and represents the exact form applicable to the corresponding linear circuit. The term in θ represents the

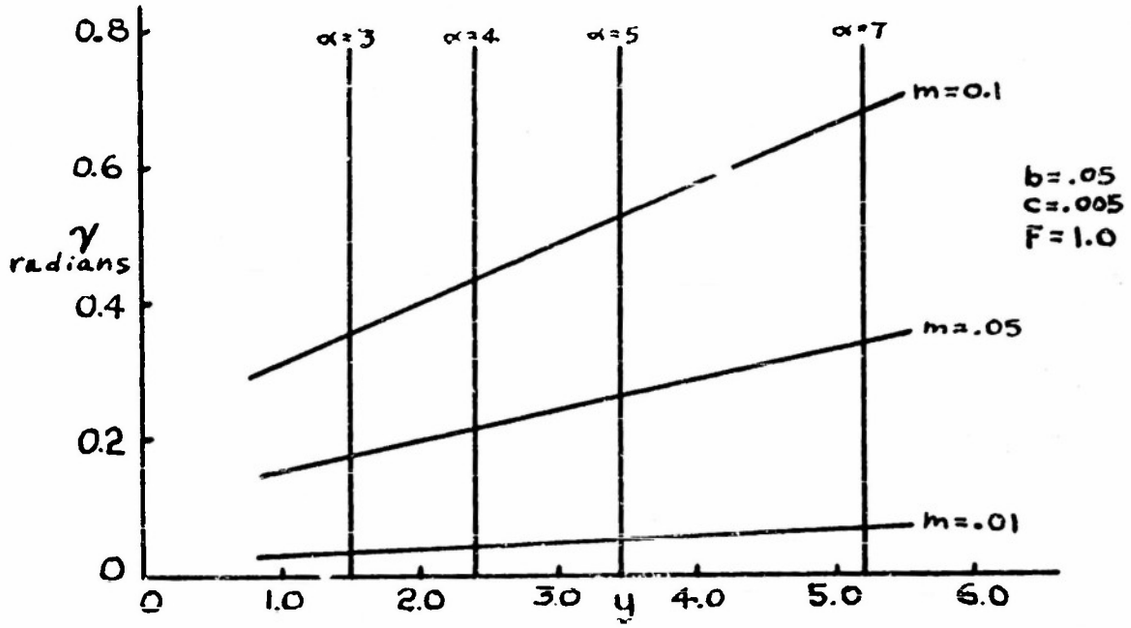

Fig. 7. Contours of constant α and constant m for $\phi_0 = \phi_s, \gamma \neq 0$.

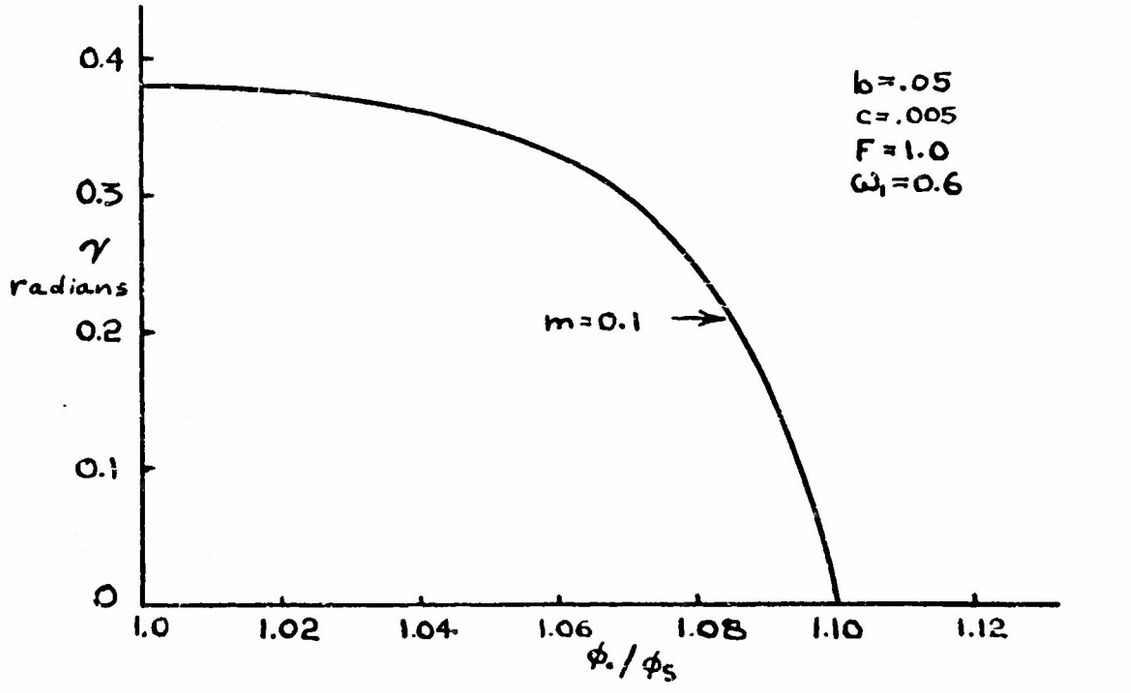

Fig. 8. Curve showing the combinations of γ and ϕ_0/ϕ_s leading to m=0.1.

steady-state part of the solution at the frequency of the excitation and the term in $\frac{\theta}{h}$ represents the transient part of the solution at a frequency related to the excitation frequency by the factor h. The development here is for the case of introducing the triggering pulse of flux at the correct time in the excitation cycle but with an amplitude slightly different from that which would lead to a transient-free solution.

By successive differentiation of Eq. (41), cubing, and substitution into Eq. (5b) with the neglect of second and third harmonic terms, it is determined that

$$\left[-\phi_\ell - \frac{F}{\omega_1^2} + \frac{b\phi_\ell}{\omega_1^2} + \frac{3c\phi_\ell^3}{4\omega_1^2} + \frac{3c\phi_\ell^3 g^2}{2\omega_1^2}\right]\cos\theta$$

$$+\left[-\frac{g\phi_\ell}{h^2} + \frac{bg\phi_\ell}{\omega_1^2} + \frac{3cg\phi_\ell^3}{2\omega_1^2} + \frac{3cg^3\phi_\ell^3}{4\omega_1^2}\right]\cos\frac{\theta}{h} = 0 \qquad (42)$$

By requiring that $g \ll 1.0$, it is seen that the term in Eq. (42) involving $\cos\theta$ requires that $\phi_\ell \approx \phi_s$, where ϕ_s is the value for the stable solution on the right-hand branch of the curve in Fig. 3. From the term in Eq. (42) involving $\cos\frac{\theta}{h}$, the following relation is established.

$$-\frac{1}{h^2} + \frac{b}{\omega_1^2} + \frac{3c\phi_s^2}{2\omega_1^2} + \frac{3cg^2\phi_s^2}{4\omega_1^2} = 0 \qquad (43)$$

If $g \ll 1.0$ this equation reduces to

$$h^2 = \frac{2\omega_1^2}{2b + 3c\phi_s^2} \qquad (43a)$$

and thus the frequency of the transient part of the solution is independent of g, the factor that expresses the difference in actual pulse magnitude from the magnitude needed for a transient-free solution. It may be noted that a larger value for the $c\phi_s^2$ product leads to a smaller value of h and thus to a higher value for the frequency of the transient component of the solution.

IV. Operation with Damping

1. Neighborhood of upper stable state.

The differential relation applicable is that of Eq. (5b) with the addition of the term $\frac{a}{\omega_1}\frac{d\phi}{d\theta}$ to the left-hand side of the equation. By the assumption of the same general form of solution as in Section II. 1., Eq. (12) is thus modified by the addition of the term

$$\frac{a}{\omega_1}\left(-A \sin \beta \frac{d\beta}{a\theta} + \cos \beta \frac{dA}{d\theta}\right) \qquad (44)$$

to the left-hand side. The magnitude function A and the phase function β are assumed to have the same form as in Eqs. (13) and (14) respectively, but now n and m are allowed to be functions of θ. The development here is for the case of $\phi_c \neq \phi_s$ and $\gamma = 0$. Thus $\psi = 90$ degrees and the following relations are valid.

$$A = \phi_1\left[1 + m \cos \frac{\theta}{\alpha}\right] \qquad (13a)$$

$$\beta = \theta + n \sin \frac{\theta}{\tau} \qquad (14a)$$

$$\frac{dA}{d\theta} = -\frac{\phi_1 m}{\alpha} \sin\frac{\theta}{\alpha} + \phi_1 \frac{dm}{d\theta} \cos\frac{\theta}{\alpha} \tag{45}$$

$$\frac{d^2A}{d\theta^2} = -\frac{\phi_1 m}{\alpha^2} \cos\frac{\theta}{\alpha} - \frac{2\phi_1}{\alpha} \frac{dm}{d\theta} \sin\frac{\theta}{\alpha} \tag{46}$$

$$\frac{d\beta}{d\theta} = 1 + \frac{n}{\alpha} \cos\frac{\theta}{\alpha} + \frac{dn}{d\theta} \sin\frac{\theta}{\alpha} \tag{47}$$

$$\frac{d^2\beta}{d\theta^2} = -\frac{n}{\alpha^2} \sin\frac{\theta}{\alpha} + \frac{1}{\alpha} \frac{dn}{d\theta} \cos\frac{\theta}{\alpha} + \frac{dn}{d\theta} \cos\frac{\theta}{\alpha} \tag{48}$$

$$\left(\frac{d\beta}{d\theta}\right)^2 = 1 + \frac{2n}{\alpha} \cos\frac{\theta}{\alpha} + \frac{2dn}{d\theta} \sin\frac{\theta}{\alpha} \tag{49}$$

The damping has been assumed to be small in the development of these relations. This assumption allows the steady-state portion of the solution to be approximately in phase with the excitation as has been assumed and allows the neglect of the terms in $\frac{d^2m}{d\theta^2}$, $\frac{d^2n}{d\theta^2}$, and $\left(\frac{dn}{d\theta}\right)^2$ which would otherwise appear in the above relations. Also it has been assumed that n is small as compared to unity so terms in n^2 have been neglected. These relations are substituted into the modified form of Eq. (12) and the resulting expression expanded by simple multiplication. In this expansion, Eqs. (21) through (26) have been used and all terms in n^2, m^2, nm, $n\frac{dn}{d\theta}$ and $m\frac{dm}{d\theta}$ have been neglected. The coefficients of the $\cos\theta \sin\frac{\theta}{\alpha}$ and the $\cos\frac{\theta}{\alpha} \sin\theta$ terms in this expansion must be separately equal to zero. This results in

$$\frac{1}{\alpha} \frac{dn}{d\theta} + \frac{dn}{d\theta} + \frac{2dm}{d\theta} + \frac{an}{\alpha\omega_1} + \frac{am}{\omega_1} = 0 \tag{50}$$

and

$$\frac{2}{\alpha} \frac{dm}{d\theta} + \frac{2dn}{d\theta} + \frac{an}{\omega_1} + \frac{am}{\alpha\omega_1} = 0 \tag{51}$$

By differentiation of Eq. (34a) with respect to θ it is found that

$$\frac{dn}{d\theta} = \frac{\alpha}{2}\left(r - \frac{1}{\alpha^2}\right) \frac{dm}{d\theta} \tag{52}$$

If Eqs. (34a) and (52) are substituted into Eq. (51) to eliminate n and its derivative and the terms rearranged, it is seen that

$$\frac{dm}{d\theta}\left[\frac{2}{a} + a\left(r - \frac{1}{a^2}\right)\right] = \frac{-am}{a\omega_1}\left[1 + \frac{a^2}{2}\left(r - \frac{1}{a^2}\right)\right] \tag{53}$$

or by simplification

$$\frac{dm}{m} = -\frac{a}{2\omega_1}\, d\theta \tag{54}$$

By integration of both sides of Eq. (54) and letting $m = m_o$ at $\theta = 0$

$$\log \frac{m}{m_o} = \frac{-a}{2\omega_1}\,\theta \tag{55}$$

or

$$\frac{m}{m_o} = \varepsilon^{-\frac{a}{2\omega_1}\theta} \tag{56}$$

Thus it is established that the damping is identical with that of the corresponding linear circuit[13] so long as the various assumptions that have been made in the derivation are valid.

2. Neighborhood of lower stable state.

As in the region of the upper stable state the term $\frac{a}{\omega_1}\frac{d\phi}{d\theta}$ must be added to the left-hand side of Eq. (5b). The solution is assumed to be the same as in Section III, Eq. (41) except that g is now allowed to be a function of θ. The factor h was shown to be independent of g in Eq. (43a) and thus in this case independent of θ. After successive differentiation and neglect of the term in $\frac{d^2g}{d\theta^2}$, the assumed solution is substituted in Eq. (5b). This involves the cubing of the assumed solution during which the term in g^3 and the terms involving the second harmonic of θ and $\frac{\theta}{h}$ were neglected. After collecting terms and equating the coefficients of the $\sin \frac{\theta}{h}$

term to zero, it is seen that

$$\frac{dg}{d\theta} = -\frac{a}{2\omega_1} g \qquad (54a)$$

Thus as a first approximation the damping is identical with that in the region of the upper stable state and with that of the linear system.

V. Solution by Analog Computer

To check the validity of the derivations in the preceding sections and to present solutions in the form of actual complete time functions, Eq. (5) was programmed on a Reeves Electronic Analog Computer as shown in block diagram form in Fig. 9. The circuit and excitation constants used in obtaining the plots to be presented are $b = .05$, $c = .005$, $F = 1.0$ and $\omega_1 = 0.65$.

Figure 10 illustrates the undamped solution with $\gamma = 0$ for various values of $\frac{\phi_o}{\phi_s}$ smaller than unity. The angle γ is set equal to zero in the computer setup by letting the initial condition on integrator No. 1 in Fig. 9 be zero and placing the desired value of ϕ_o as the initial condition on integrator No. 4 with zero initial condition on integrator No. 3. The initial condition on integrator No. 2 starts the excitation at its maximum instantaneous value at $t = 0$. It can be seen from the plots in Fig. 10 that m and n vary in the expected fashion and that α is essentially independent of m in this region. As calculated by Eq. (31a), $\alpha = 3.75$ which checks the computer solution fairly accurately as is obvious by comparison of the plots of ϕ with the plot of the excitation on the same time scale. It is apparent in Fig. 10 that angle ψ is 90 degrees.

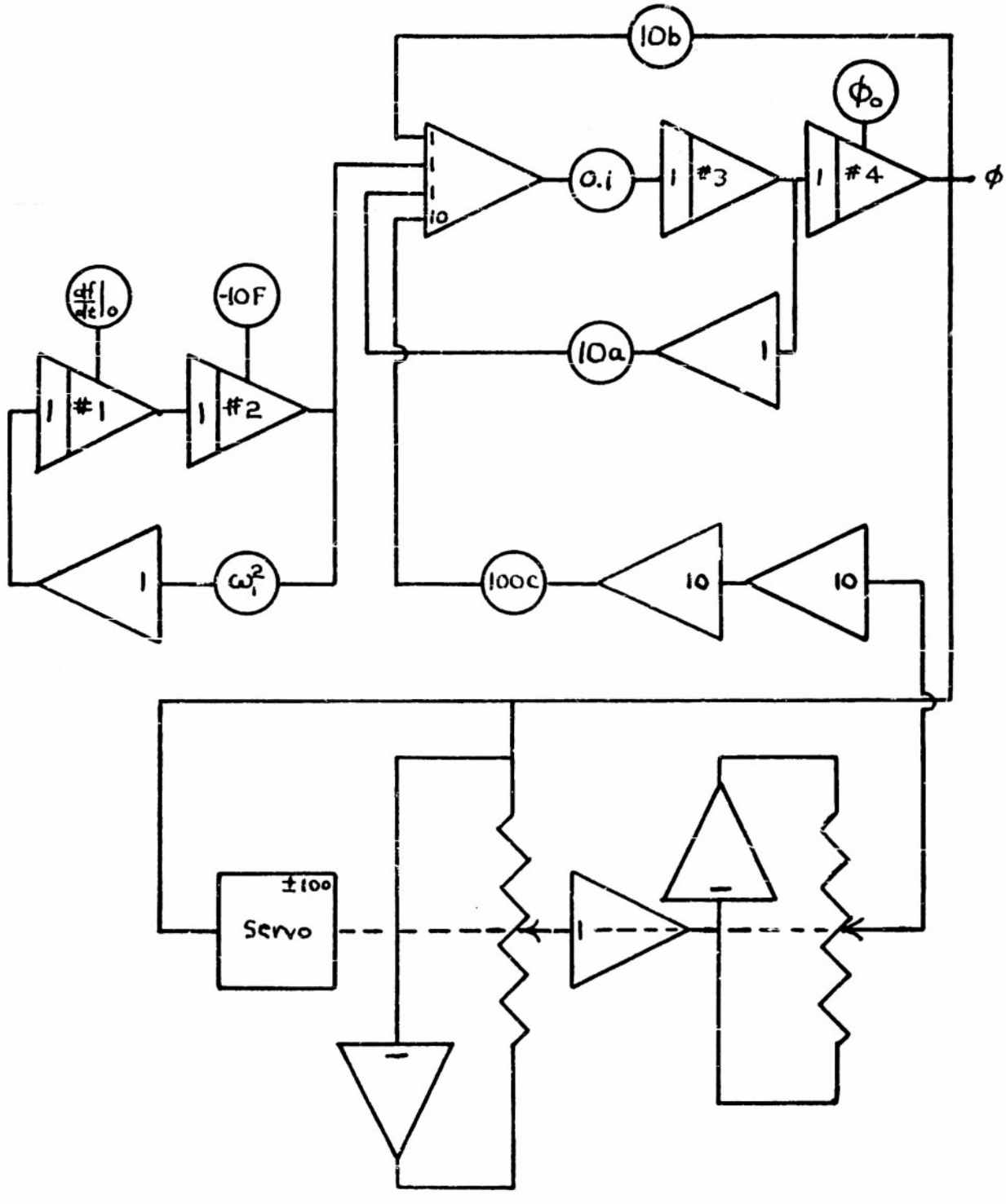

Fig. 9. Analog computer setup for solving Eq. (5).

Captions for Figs. 10-15

These figures are all solutions for Eq. (5) obtained with the analog computer setup of Fig. 9 under the following conditions.

Fig. 10. $\phi_o/\phi_s < 1.0$, $\gamma = 0$, upper stable state.

Fig. 11. $\phi_o/\phi_s > 1.0$, $\gamma = 0$, upper stable state.

Fig. 12. $\phi_o/\phi_s > 1.0$, $a \neq 0$, upper stable state.

Fig. 13. $\phi_o/\phi_s = 1.0$, $\gamma \neq 0$, upper stable state.

Fig. 14. $g \neq 0$, $\gamma = 0$, lower stable state.

Fig. 15. $\phi_o/\phi_s \neq 1.0$, $\gamma = 0$, $a \neq 0$, upper stable state.

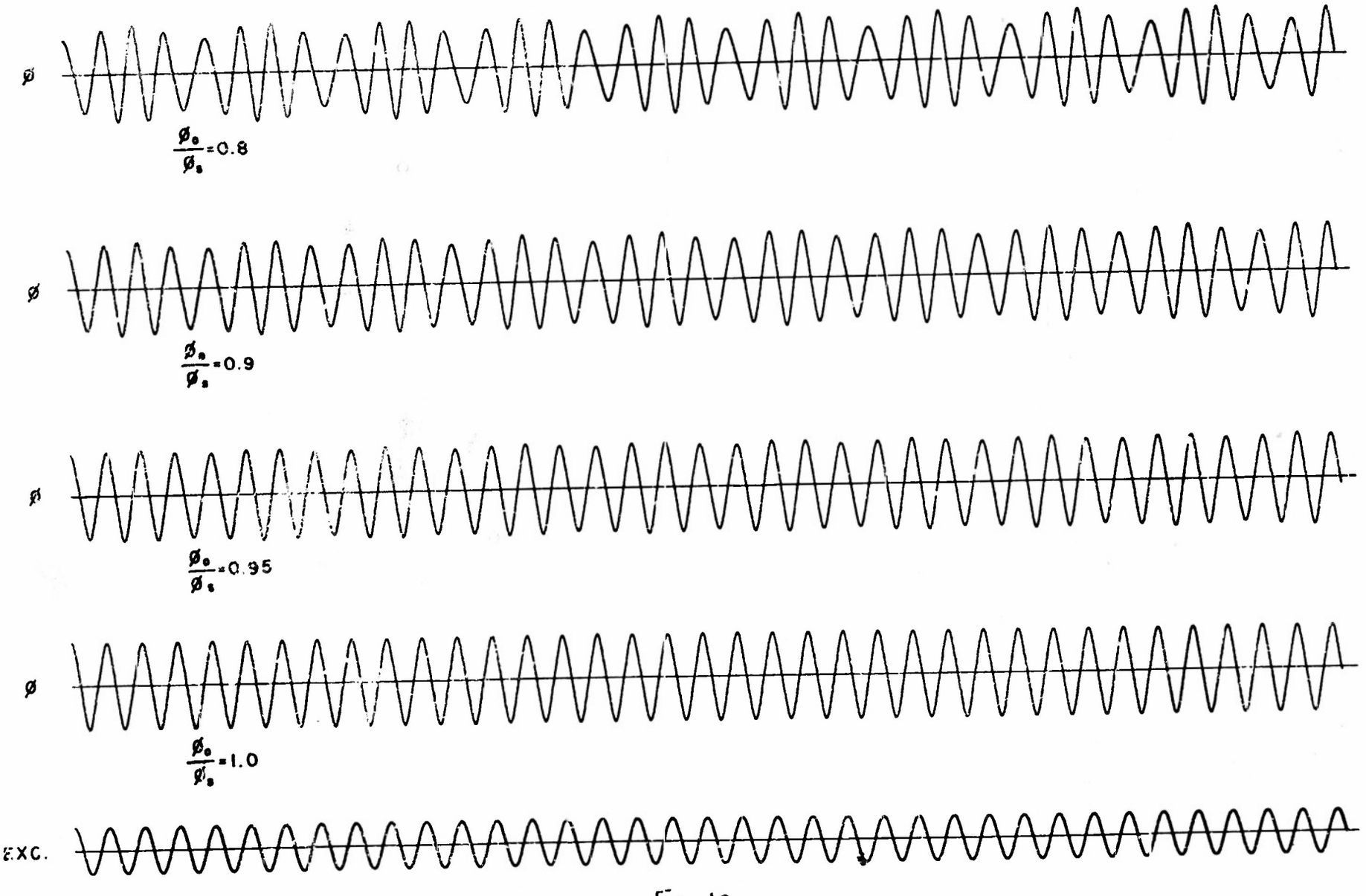
ø
$\frac{\phi_0}{\phi_s}$=0.8
ø
$\frac{\phi_0}{\phi_s}$=0.9
ø
$\frac{\phi_0}{\phi_s}$=0.95
ø
$\frac{\phi_0}{\phi_s}$=1.0
EXC.

Fig. 10

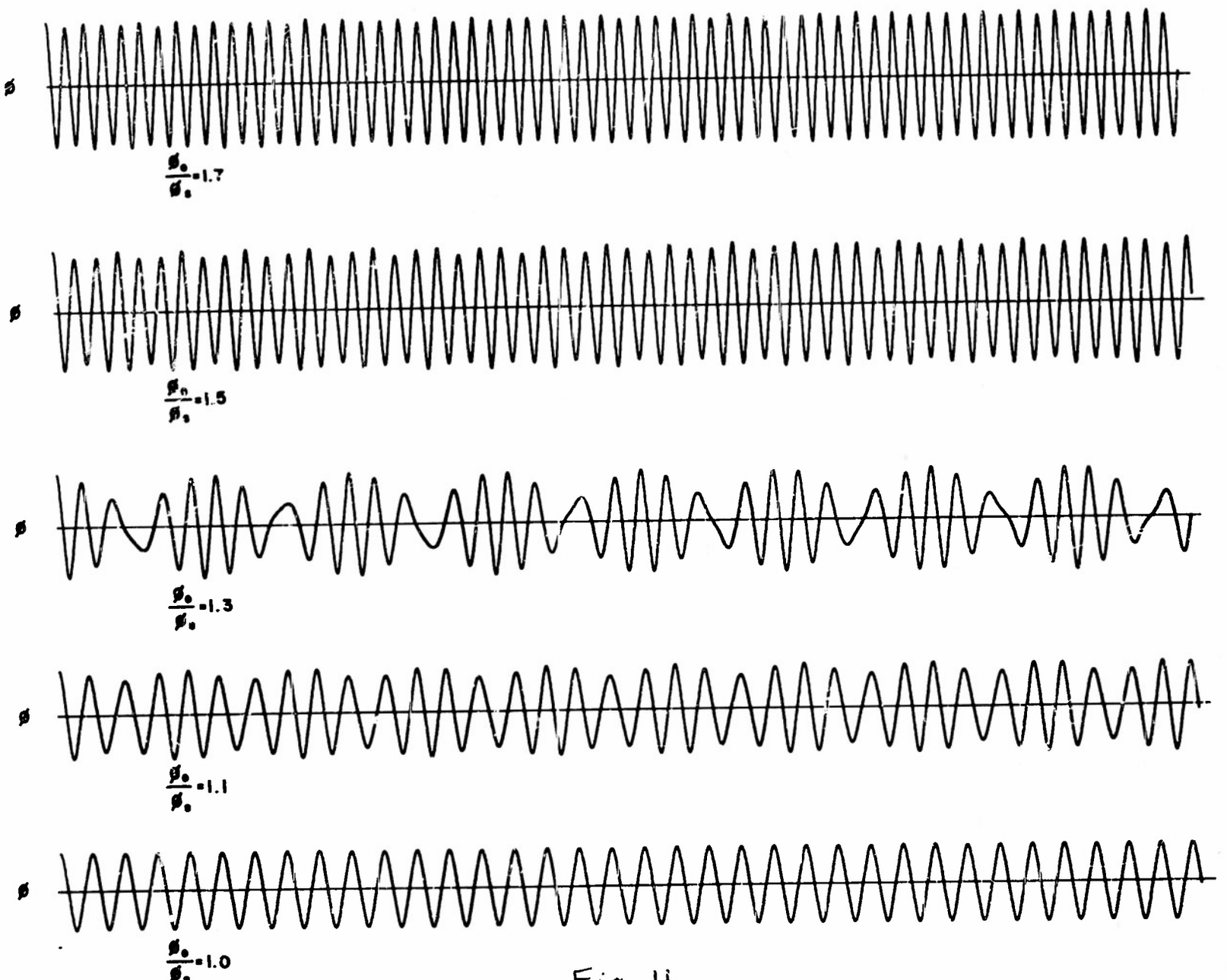
ϕ
$\frac{\beta_0}{\beta_1}=1.7$
ϕ
$\frac{\beta_0}{\beta_1}=1.5$
ϕ
$\frac{\beta_0}{\beta_1}=1.3$
ϕ
$\frac{\beta_0}{\beta_1}=1.1$
ϕ
$\frac{\beta_0}{\beta_1}=1.0$

Fig. 11

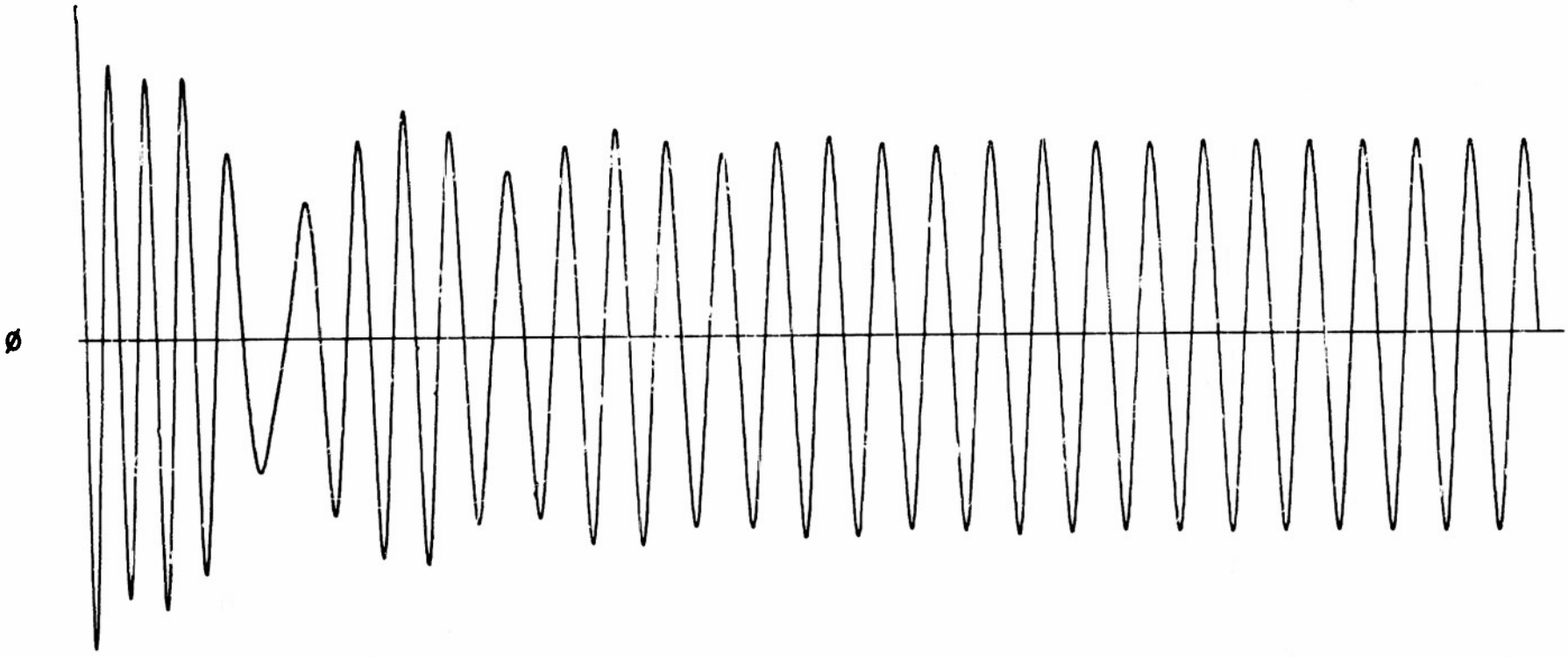

Fig. 12

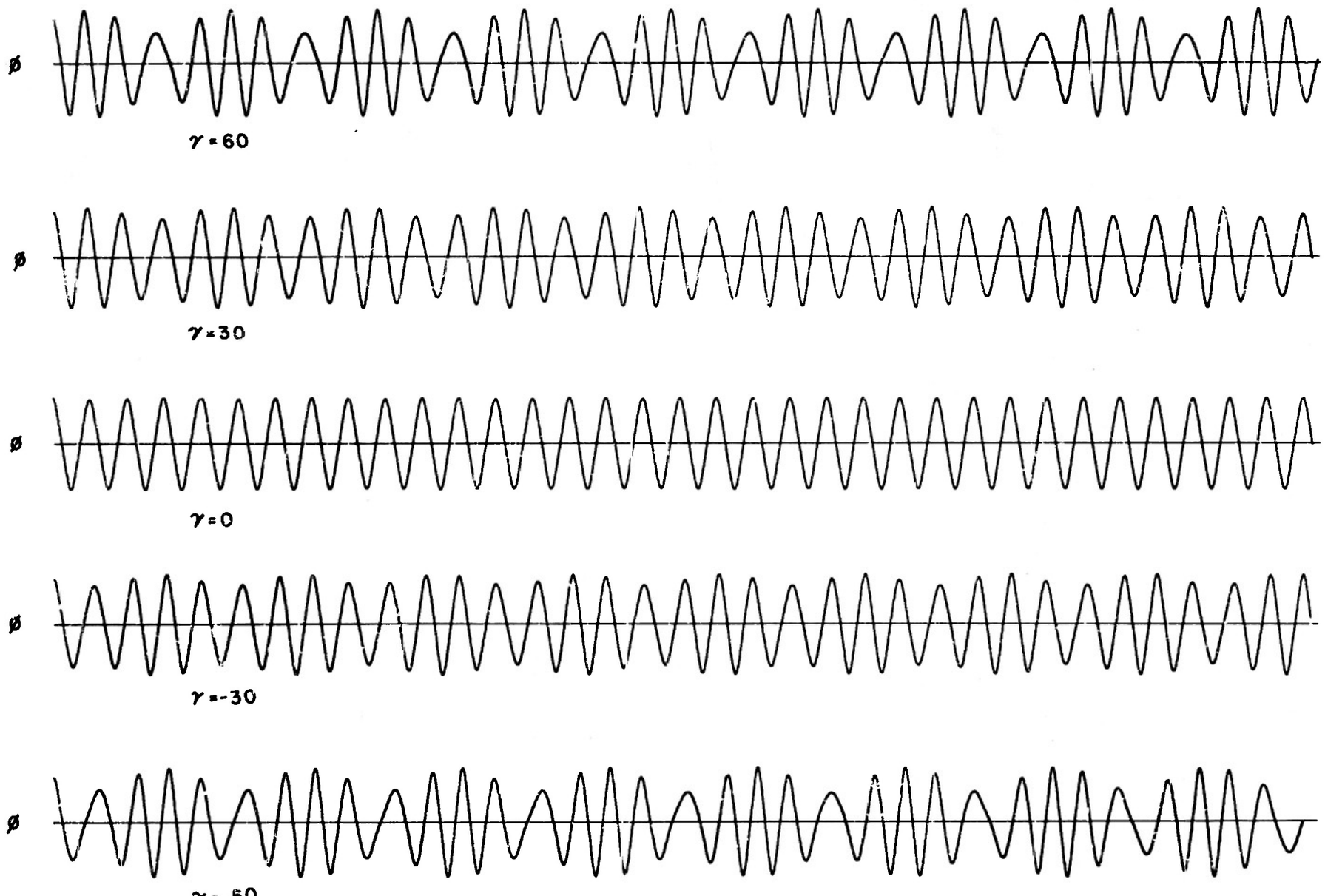

Fig. 13

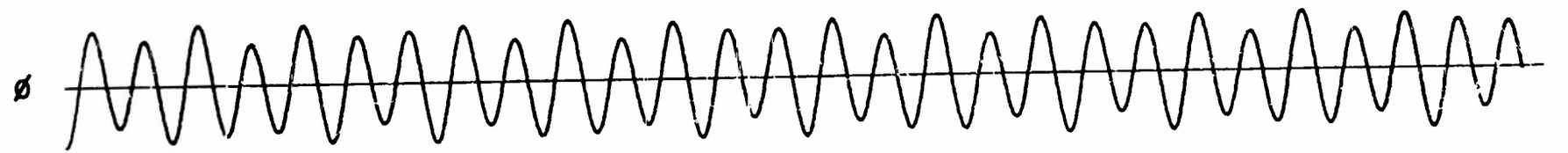

g = 0.2

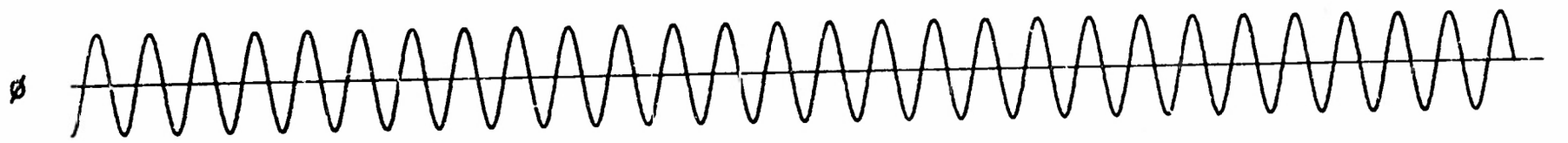

g = 0

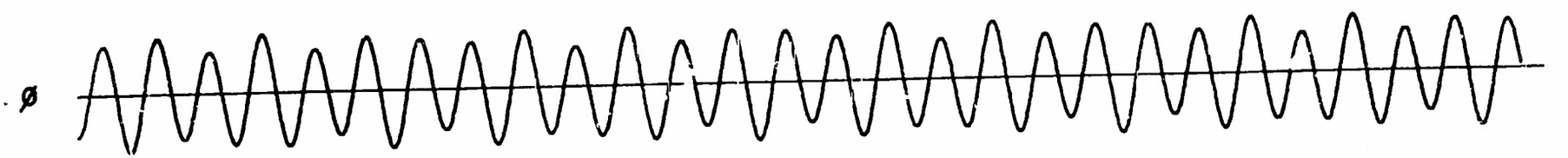

g = - 0.2

Fig. 14

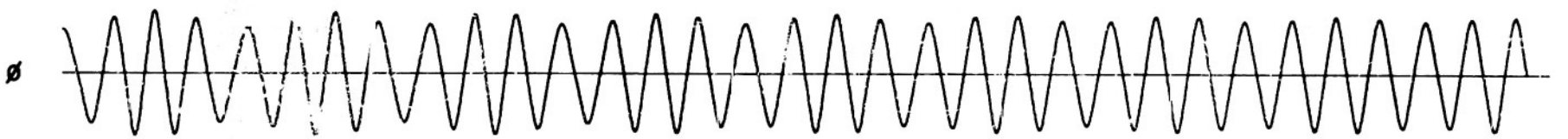

a=.01

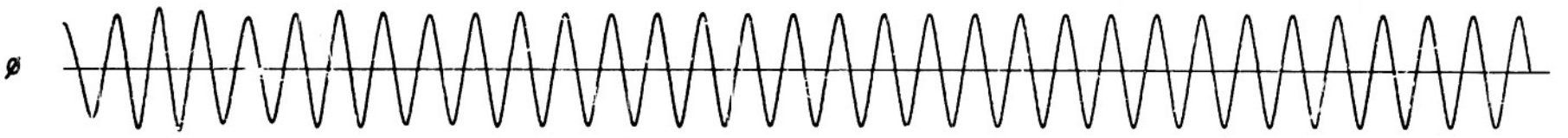

a=.05

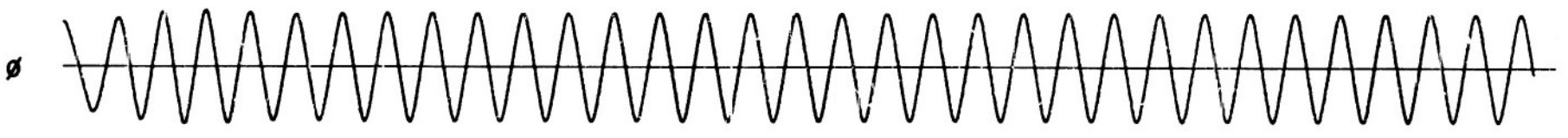

a=0.1

Fig. 15

Figure 11 shows the nature of the solution for the same situation as above except for values of $\frac{\phi_o}{\phi_s}$ greater than unity. Here the transfer to the region where the solution is determined almost entirely by the high-frequency transient is clearly demonstrated. It is also apparent that α increases somewhat from its value in Fig. 10 as ϕ_o is increased as predicted in Section II. 3.

To illustrate the nature of the solution in an actual physical system where damping is inherently present, the above constants were used with the addition of $a = .05$. The resulting plot is shown in Fig. 12. The initial condition ϕ_o was chosen large so the solution starts off essentially as a high-frequency transient with an exponential decay. As soon as the amplitude decays somewhat, the modulation of amplitude and phase appears, and subsequently the transient portion of this is damped out leaving what is essentially a sinusoid representing the upper steady-state solution. This is the general behavior that is predicted qualitatively by an inspection of the various regions and curves in Fig. 6. There is no assurance that the upper stable state will be reached in the above procedure. Slightly different methods of obtaining a plot of the form of Fig. 12 have led to the final operation being at the lower stable state. This possibility is illustrated by Hayashi[10] in a curve, for a particular set of circuit and drive constants, indicating that certain values of ϕ_o may lead eventually to operation at either of the two stable states depending on the value of the angle γ.

The operation with $\frac{\phi_o}{\phi_s} = 1.0$ and $\gamma \neq 0$ is shown in Fig. 13. The desired value for γ is placed into the computer setup by adjusting the initial condition on integrator No. 2 to the instantaneous value

of the excitation consistent with the desired value of γ and placing an initial condition on integrator No. 1 of sufficient magnitude to insure that F has the desired value, F = 1.0. The theory developed in Section II. 5. is not valid for values of γ as large as shown in some of the plots in Fig. 13 but, for example, the value of α as calculated from Eq. (31a) is approximately correct so long as γ is small, and the plots show that α increases slightly as γ is increased. This would be predicted by including the n^2 and m^2 terms in the analysis of Section II. 5. It may be observed that $\psi = 0$ in these plots.

The undamped solution in the neighborhood of the lower stable state is shown in Fig. 14. Here the modulation of amplitude and phase does not occur in the same manner as in the neighborhood of the upper stable state but, as developed in Section III, the solution is in the form of the sum of two sinusoidal components. The plots of Fig. 14 indicate that the frequencies of the two components have a ratio of almost two to one. Calculations using Eq. (43a) give h = 1.9.

Figure 15 illustrates the effect of damping on the solution for $\frac{\phi_o}{\phi_s} = 0.8$ and $\gamma = 0$. Here a = .01, a = .05 and a = 0.1 respectively for the three curves shown. Calculations of the expected behavior for a = .05 using Eq. (56) indicate that the amplitude modulation should decrease to about one-third after about five cycles of the excitation. This general behavior can be seen in the curve for a = .05 in Fig. 15.

VI. Experiment with Actual Inductor

The circuit of Fig. 1 was established using the 115-volt winding of a Western Electric transformer No. D163413 as the iron-cored inductor. The core of this unit is designed to operate at 400 cps. It has a relatively small cross-section and is easily saturated. The capacitance used was $C = 1.0\ \mu f$ and the resistance of about 500 ohms is that due to the winding resistance and core loss of the inductor.

The constants describing the inductor were evaluated previously by means of a method presented in the literature.[14] Briefly the method used was to present a hysteresis loop of controllable size on the screen of a calibrated oscilloscope. The magnetization curve is then determined by connecting the tips of the various hysteresis loops and the desired constants of Eq. (1) were determined by a curve-fitting procedure. For the present inductor,

$$b = \frac{a_1}{C} = \frac{10^6}{7.2} = 1.39 \times 10^5 \text{ sec}^{-2}$$

and

$$c = \frac{a_3}{C} = 1.2 \times 10^8 \text{ weber-turns}^{-2} \text{ sec}^{-2}$$

where a_1 is the reciprocal of the self-inductance of the corresponding linear inductor and a_3 is the nonlinearity parameter of Eq. (1).

If the circuit is supplied with 15 volts rms at 200 cps, $F = \omega_1 E = 2.66 \times 10^4$ and the value of y is

$$y = \left(\frac{\omega_1^2}{b} - 1\right) \frac{b}{F^{2/3} c^{1/3}} = 3.25$$

From Fig. 3, $x = 2.3$ for the upper stable state. From Fig. 4,

$$\left(\frac{\omega_1^2}{F^{2/3} c^{1/3}}\right) r = 8 \quad \text{or} \quad r = 2.3$$

and

$$\left(\frac{\omega_1^2}{F^{2/3}\,c^{1/3}}\right)s = .44 \quad \text{or} \quad s = .125$$

Then from Fig. 5 or Eq. (31a), $\alpha = 4.7$.

If the triggering pulse of flux in this circuit is adjusted so $\frac{\phi_o}{\phi_s} = 1.1$ and $\gamma = 0$, it is seen that $m = 0.1$ from Eq. (32a), and from Eq. (34a) that

$$n = \frac{\alpha m}{2}\left(\pi - \frac{1}{\alpha^2}\right) = \frac{4.7 \times 0.1}{2}\left(2.3 - \frac{1}{22}\right) = 0.53 \text{ radians.}$$

The maximum instantaneous frequency in the waveform of the solution is gained by the differentiation of Eq. (14) with respect to time and is $\omega_1\left(1 + \frac{n}{\alpha}\right)$. Substitution of the above values in this expression indicates that the maximum instantaneous frequency for the above condition of operation is about 11-percent higher than the excitation frequency.

If now the pulsing conditions are altered to allow $\frac{\phi_o}{\phi_s} = 1.0$ and $\gamma = 0.2$, it is seen that $n = 0.2$ from Eq. (32b) and from Eq. (34a), $m = .038$. Thus the introduction of a triggering pulse of amplitude equal to ϕ_s at a time corresponding to 11.5 degrees from the time of the peak of the excitation leads to an amplitude at the peak of the modulation about 4-percent greater than the amplitude of the steady-state solution alone.

If the pulsing condition is further altered to allow $\frac{\phi_o}{\phi_s} \neq 1.0$ and $\gamma \neq 0$, Eqs. (32) and (33) must be used. It is assumed for the sake of illustration that the amplitude-modulation index is desired to be $m = 0.1$ for $\gamma = 0.2$. Substitution of known values in Eq. (33) gives

$$\tan(0.2 - 0.53\cos\psi) = \frac{.0213\cos\psi}{(1 + .1\sin\psi)(1 + .11\sin\psi)}$$

By a trial-and-error procedure ψ is found to be approximately 69 degrees. Substitution of this value, along with the other known values, into Eq. (32) shows that

$$\frac{\phi_o}{\phi_s} = (1 + 0.1 \sin 69^\circ) \cos (0.2 - 0.53 \cos 69^\circ) = 1.09$$

In other words if a pulse magnitude 9-percent greater than ϕ_s is inserted in the system at such a time that $\gamma = 0.2$, an amplitude modulation corresponding to the assumed $m = 0.1$ will occur. This does not does not represent a large difference from the calculation above for $\gamma = 0$ but the difference increases rapidly as γ is made larger, as can be seen from an inspection of Fig. 8.

According to the development in Section III, the frequency of the transient component generated in the above circuit in the neighborhood of the lower stable state is expressed by Eq. (43a). At the lower stable state for $y = 3.25$, the value of x from Fig. 3 is $x = 0.32$ and since $\phi_s = (\frac{F}{c})^{1/3} x = 1.9 \times 10^{-2}$, it is seen that

$$h^2 = \frac{2\omega_1^2}{2b + 3c\phi_s^2} = \frac{2(2\pi \cdot 200)^2}{2 \quad 1.39 \times 16^5 + 3 \cdot 1.25 \times 10^8 \, (1.9 \times 10^{-2})^2} = 9.8$$

Thus $h = 3.11$ so approximately 3 cycles of the excitation occur during one cycle of the low-frequency transient.

The laboratory setup used in testing the actual circuit is shown in Fig. 16. The triggering pulse is introduced in the two low-voltage windings of the transformer connected in series. The inductor voltage is integrated by means of R_1 and C_1 so the voltage across C_1 has approximately the form of the flux wave in the core. A delayed trigger from the oscilloscope is used to actuate a relay which in turn

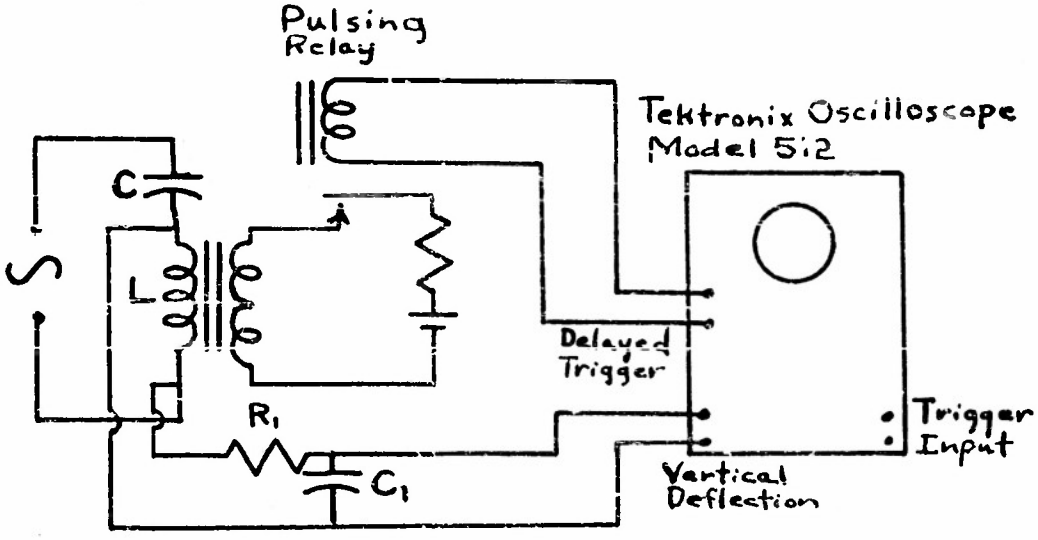

Fig. 16. Laboratory setup used in testing circuit of Fig. 1.

actuates the circuit applying a pulse to the low-voltage windings. This is not directly a pulse of flux as described in the previous sections but nevertheless results in flux being established in the core. The time during which this pulse exists and its relative magnitude are clearly evident in the oscillographic traces reproduced in Figs. 17 and 18. The pulsing circuit may be adjusted to release the system at various times in the excitation cycle. As Rayment[10] has developed, this may lead to a steady-state solution at either of the two stable states depending on the time of release. Transients leading to final operation at the upper stable state are shown in Fig. 17. The modulation of amplitude is clearly visible although it is quickly damped out. The modulation of phase, difference in spacings of zero crossings, is not visible in a tracing of this size. Transfers to the lower stable state after the release of the system by the pulsing circuit are shown in Fig. 18. The transient behavior here is clearly that of the sum of two sinusoidal components with the [illegible] being rapidly attenuated. The various traces in Figs. 17 and 18 are for slightly different magnitudes of pulse and for different times of termination of the pulse with respect to the peak of the excitation voltage of the circuit.

The oscillograph trace of Fig. 18(f) shows the voltage across the inductor instead of the flux in the core. Here the effect of neglecting the third harmonic terms in the analysis can be seen by observing the tendency toward a flat-topped wave in the region of the upper stable state. The effect of the third-harmonic is more pronounced in the waveform of the voltage than in the waveform of flux

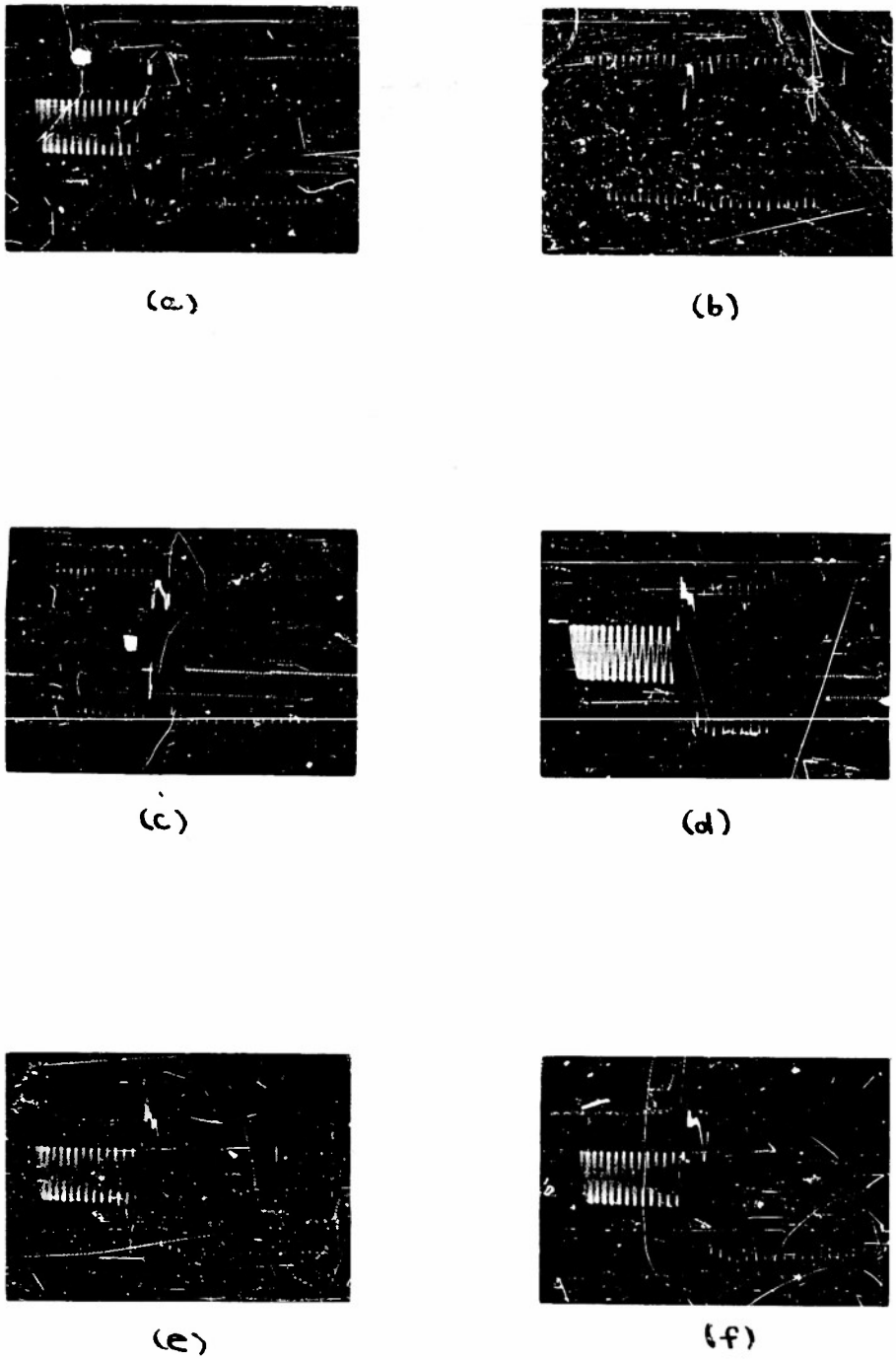

Fig. 17. Oscilloscope traces of response in the neighborhood of the upper stable state.

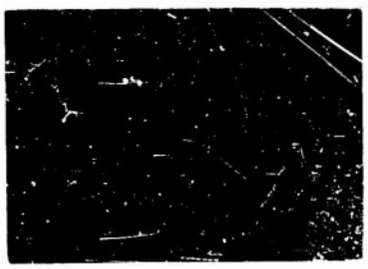

(a)

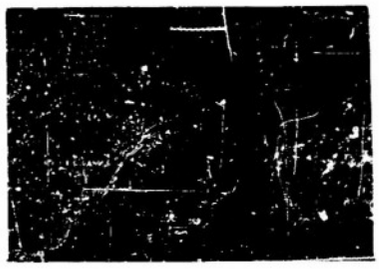

(b)

(c)

(d)

(e)

(f)

Fig. 18. Oscilloscope traces of response in the neighborhood of the lower stable state.

in Figs. 17 and 18 because the inductor voltage is the derivative of the flux and thus harmonics are accentuated in the waveform of voltage. Alternatively, harmonics are suppressed by the integrator circuit of R_1 and C_1 acting as a low-pass filter. As stated previously, the nonlinearity is not so important in the region of the lower stable state so the inductor voltage in Fig. 18(f) appears much more sinusoidal in this region.

While it is difficult to obtain quantitative data from these oscilloscope traces, it is felt that they indicate qualitatively the nature of the solution predicted in the foregoing analysis.

VII. General Comments

The transfer from the upper to the lower stable state in a circuit as shown in Fig. 1 is somewhat different from the transfer in the opposite direction. If the triggering pulse of flux releases the system in the region of the lower stable state, $g \ll 1.0$, and the operation is characterized by a solution in the form of the sum of two sinusoidal waves of different amplitude and frequency. If the triggering pulse releases the system in the region of the upper stable state, $m \ll 1.0$, and operation is characterized by a solution in the form of a combined amplitude and phase-modulated wave, so long as the approximations involved in the analysis are valid. These approximations require that $\frac{\phi_o}{\phi_s}$ be close to unity and that γ be close to zero.

The discussion to this point has been directed largely toward the simple circuit of Fig. 1. In a complete ferroresonant trigger circuit involving two circuits of the form shown in Fig. 1 the operation is

somewhat more complicated since transfers in both directions take place during the same time interval and the behavior of one half of the circuit affects the other because of the common impedance. However it seems reasonable to assume that as a first approximation the transient which independently is of the longer duration will determine the time of the over-all transfer. The ideal condition of operation would require using a pulsing system that would establish exactly the correct condition of flux in both cores at exactly the correct time in the excitation cycle. Then $\frac{\phi_o}{\phi_s} = 1.0$ and $\gamma = 0$ in one core and $g = 0$ in the other and there would be no transient generated. The transition time would then be that of the length of the pulse itself. This condition is undoubtedly very difficult to achieve in a practical circuit. However if an appreciable transient generated as a result of an incorrect pulsing condition is still present after four or five cycles of the excitation, it would appear advantageous to delay the time position of the triggering pulse enough to allow a smaller-magnitude transient to be generated. It should be noted that this procedure would increase the complexity of the pulsing circuit to a considerable degree.

An alternate pulsing system of even more complex nature is that which introduces the pulse of flux at the wrong time in the excitation cycle, $\gamma \neq 0$, but which has a magnitude equal to the instantaneous magnitude of the steady-state value of flux. Here the pulsing circuit must adjust the rate of change of flux $\frac{d\phi}{d\theta}$ at the time of the release of the system by the pulse to that consistent with the $\frac{d\phi}{d\theta}$ of the steady-state solution at that instant. This leads to a transient-free

operation in the same fashion as in the case of $\frac{\phi_o}{\phi_s} = 1.0$ and $\gamma = 0$ and allows the triggering pulse to occur at any time in the excitation cycle at the expense of an extremely complex pulsing circuit.

With a pulsing condition different from the ideal conditions outlined above and thus leading to a certain magnitude of transient, the damping may be adjusted to cause the transient component to disappear as quickly as possible. Some general conclusions may be drawn regarding the best point of operation along the curve of Fig. 3 if the damping is to be adjusted to decrease the transition time. If the inductor has been chosen, b and c are fixed but operation may be shifted along the normalized-frequency axis of Fig. 3 by changing the excitation frequency, ω_1. The effect of damping puts an upper limit on the value of excitation frequency that will lead to the existence of two stable states. It may be shown[7] that Eq. (7) may be rewritten as

$$\left[\phi_s(b - \omega_1^2) + \frac{3}{4} c\phi_s^3\right]^2 + a^2\phi_s^2\omega_1^2 = F^2 \qquad (57)$$

to include the effects of damping. By differentiation with respect to ϕ_s and setting $\frac{d\omega_1}{d\phi_s}$ equal to zero,

$$\left[(b - \omega_1^2) + \frac{3}{4} c\phi_s^2\right]\left[(b - \omega_1^2) + \frac{9}{4} c\phi_s^2\right] + a^2\omega_1^2 = 0 \qquad (58)$$

This equation established the locus of the vertical tangents to the response curves of the form of Fig. 2 but which include the effect of damping. If this equation of the locus of vertical tangents is differentiated with respect to ϕ_s and again $\frac{d\omega_1}{d\phi_s}$ set equal to zero, the condition of operation where only one point of vertical tangency, and thus one stable state, exists should be established. The result

of this operation in terms of the normalized quantities x and y is

$$y = \frac{9}{8} x^2 \tag{59}$$

By substituting this relation into the normalized form of Eq. (57) the following relation is gained.

$$\frac{y^2}{9} + \frac{a^2(yF^{2/3}c^{1/3} + b)}{c^{2/3}F^{4/3}} = \frac{9}{8y} \tag{60}$$

This equation establishes the relation between the normalized excitation frequency y and the damping a to cause the two stable states to merge. It is evident from inspection of Fig. 3 that the minimum value of y in Eq. (60) must be approximately $y = 1.7$. Experiment with the actual inductor mentioned in Section VI gave a value of about $y = 1.8$. Here external series resistance was added until the two stable states merged at a drive frequency of about 140 cps as the drive voltage was kept at 15 volts rms. Substitution of the value $y = 1.7$ into Eq. (60) allows the calculation of ' · approximate magnitude of the maximum permissible value for the damping constant once the excitation constants and the circuit constants are fixed. This amount of damping coupled with the appropriate drive frequency leads to the most rapid attenuation of the transient oscillations and thus qualitatively to the most rapid transition from one stable state to the other for a given condition of triggering. It should be noted that the above paragraphs do not take into consideration the difference in levels between the two stable states. In the limiting case discussed, the two levels are of the same amplitude.

It may be seen by inspection of Fig. 3 that higher values of ω_1 will lead to a greater difference in the amplitude of flux at the two

stable states. This may be a factor in many designs and in general it is probable that some compromise must be made between short transition time and difference in level between the two stable states. The determination of the required circuit and excitation constants to satisfy a given set of conditions is illustrated in the following paragraphs.

If the frequency of the excitation ω_1, the actual response at one of the two stable states, and the ratio of the response at the two stable states are specified, the remaining circuit constants may be computed. As an example ω_1 is chosen to be 6.28×10^4 radians/sec. The ratio of the steady-state response at the two stable states is chosen to be equal to ten. The actual voltage across the inductor is desired to be 20 volts rms when operation is at the lower stable state. For values of the above-mentioned ratio as high as ten, the inductor voltage at the lower stable state is approximately equal to the supply voltage. Thus in this example $E = 20\sqrt{2}$ volts and $F = \omega_1 E = 1.78 \times 10^6$ weber-turns/sec^2. The inductor voltage at the upper stable state is 10E or $200\sqrt{2}$ volts. Inspection of Fig. 3 indicates that for a ratio of the response at the two stable states equal to ten, y is about 4.0 and the two values of x are about 2.5 and 0.25 for the upper and lower state respectively. The inductor voltage E_L is related to the flux-linkage ϕ_s by $E_L = \omega_1 \phi_s$, so ϕ_s at the upper stable state is $\frac{200\sqrt{2}}{6.28 \times 10^4} = 4.5 \times 10^{-3}$ weber-turns. Since $x = \left(\frac{c}{F}\right)^{1/3} \phi_s$, the required value for c may be computed by substitution of the known constants into this equation. In this example

$$c = F \frac{x^3}{\phi_s^3} = \frac{1.78 \times 10^6 (2.5)^3}{(4.5 \times 10^{-3})^3} = 3.1 \times 10^{14} \text{ weber-turns}^{-2} \text{ sec}^{-2}$$

Since $y = (\frac{\omega_1^2}{b}-1)\frac{b}{F^{2/3}C^{1/3}} = 4.0$, the required value for b may be computed as $b = 1.1 \times 10^7$ sec^{-2}. This completes the evaluation of all the circuit and excitation constants for the case of zero damping.

The damping constant a should now be adjusted to be of sufficient magnitude just to allow the existence of two stable states at the chosen frequency of excitation. This adjustment will cause the most rapid decay of any transient oscillation. Introduction of the damping will decrease slightly the ratio of amplitude at the two stable states. Therefore in this example the ratio will be slightly less than ten after the addition of damping. The procedure used to determine the value of the damping constant a is to solve Eqs. (57) and (58) simultaneously. Equation (57) is the equation for the steady-state response including the effect of damping. Equation (58) is the equation for the locus of the vertical tangents to the response curves. After substitution of the constants already determined for the undamped case, Eqs. (57) and (58) are equations in the two variables, the damping constant a and the steady-state response ϕ_s. The numerical calculation required to eliminate ϕ_s and solve for the damping constant a is lengthy and is not included here. However the result of such a calculation indicates that the approximate value needed to satisfy the stated requirements for the damping in this particular circuit is $a = 6.9 \times 10^3$ sec^{-1}.

The calculations above have indicated a design procedure starting with a particular set of requirements. If a large ratio between the two stable states and large damping are both desired results, it is possible that the design procedure should be based on a figure of merit defined as the product of these two quantities. In particular, the

excitation frequency should be chosen to allow this product to be as large as possible. As stated previously, Eq. (58) is the equation for the locus of the vertical tangents to the response curves which include the effect of damping. It has been shown[7] that if the factor $\left[(b - \omega_1^2) + \frac{3}{4} c\phi_s^2\right]$ of Eq. (58) is set equal to zero, the resulting equation determines, approximately, the locus of the vertical tangents which occur at the high-amplitude stable state. This is the stable state of interest when the damping is to be increased until any further increase would result in the existence of only one stable state at a particular excitation frequency. Substitution of the above relation into Eq. (57), the equation for the steady-state response including the effect of damping, results in the relation $a\phi_s\omega_1 = F$. Since $F = \omega_1 E$, it is seen that ϕ_s at the upper stable state is given by $\frac{E}{a}$. Here E is the amplitude of the supply voltage and a is the maximum allowable damping constant. It has been stated previously that the ϕ_s at the lower stable state is given by $\frac{E}{\omega_1}$ if the ratio of the amplitude at the two stable states is reasonably large. This is equivalent to having $\omega_1^2 \gg b$. From the above relations at the two stable states, it is seen that the ratio of the amplitude at the upper stable state to the amplitude at the lower stable state is equal to $\frac{\omega_1}{a}$. This ratio multiplied by the damping constant is equal to ω_1. Thus it appears that ω_1 should be chosen as high as possible to obtain a maximum value for the figure of merit defined above. Once ω_1 is chosen, the determination of the remaining circuit and excitation constants would proceed as in the previous example.

Bibliography

1. C. G. Suits, "Studies in Nonlinear Circuits," Trans. AIEE, 50, 724, (1931).
2. C. G. Suits, "Nonlinear Circuits for Relay Application," Electrical Engineering, 50, 936, (1931).
3. P. H. Odessey and E. Weber, "Critical Conditions in Ferroresonance," Trans. AIEE, 57, 444, (1938).
4. C. Isborn, "Ferroresonant Flip-Flops," Electronics, 25, 121, (April, 1952).
5. R. W. Rutishauser, "Ferroresonant Flip-Flops," Electronics, 27, 152, (May, 1954).
6. J. J. Stoker, "Mathematical Methods in Nonlinear Vibration Theory," Proc. of the Symposium on Nonlinear Theory, (Polytechnic Institute of Brooklyn, New York, 1953), pg. 33.
7. J. J. Stoker, "Nonlinear Vibrations," (Interscience Publishers, New York, 1950), Chapt. 4.
8. J. J. Stoker, "Nonlinear Vibrations," (Interscience Publishers, New York, 1950), Chapt. 6.
9. R. W. Buchheim, "Systems with Nonlinear Restoring Forces," (Dissertation presented to the Graduate School of Yale University, 1953).
10. C. Hayashi, "Forced Oscillations with Nonlinear Restoring Force," J. A. P., 24, 198, (1953).
11. G. Duffing, "Erzwungene Schwingungen bei veränderlicher Eigenfrequenz," (F. Vieweg u. Sohn, Braunschweig, 1918).

12. I. S. and E. S. Sokolnikoff, "Higher Mathematics for Engineers and Physicists," (McGraw-Hill, New York, 1941), Chapt. 7.

13. K. Y. Tang, "Alternating-Current Circuits," (International Textbook Company, Scranton Pennsylvania, 1940), Chapt. 20.

14. W. J. Cunningham, "An Experiment with a Nonlinear Circuit," American Journal of Physics, 16, 382, (1948).